The time course of molecular acclimation to seawater in a euryhaline fish

Lucrezia C. Bonzi[1*], Alison A. Monroe[1], Robert Lehmann[2], Michael L. Berumen[1], Timothy Ravasi[3,4] and Celia Schunter[5*]

[1] Red Sea Research Center, Biological and Environmental Science and Engineering Division, King Abdullah University of Science and Technology, Thuwal, Saudi Arabia

[2] Biological and Environmental Sciences and Engineering Division, Computer, Electrical and Mathematical Sciences and Engineering Division, King Abdullah University of Science and Technology, Thuwal, Saudi Arabia

[3] Marine Climate Change Unit, Okinawa Institute of Science and Technology Graduate University, 1919-1 Tancha, Onna-son, Okinawa, Japan

[4] Australian Research Council Centre of Excellence for Coral Reef Studies, James Cook University, Townsville, Queensland, Australia

[5] Swire Institute of Marine Science, School of Biological Sciences, The University of Hong Kong, Pokfulam Road, Hong Kong SAR

* corresponding author

Correspondence: Lucrezia C. Bonzi (lucrezia.bonzi@gmail.com) and Celia Schunter (celiaschunter@gmail.com)

Abstract

The Arabian pupfish, *Aphanius dispar*, is a euryhaline fish inhabiting both inland nearly-freshwater desert ponds and highly saline Red Sea coastal lagoons of the Arabian Peninsula. Red Sea populations have been found to receive migrants from desert ponds that are flushed out to sea during flash floods, requiring rapid acclimation to a greater than 40 ppt change in salinity. To investigate the molecular pathways of salinity acclimation during such colonization events, a Red Sea coastal lagoon and a desert pond population were sampled, with the latter exposed to a rapid increase in water salinity. Changes in branchial gene expression were investigated via genome-wide transcriptome measurements over time from 6 hours to 21 days. The two natural populations displayed basal differences in genes related to ion transport, osmoregulation and immune system functions. These mechanisms were also differentially regulated in seawater transferred fish, revealing their crucial role in long-term adaptation. Other processes were only transiently activated shortly after the salinity exposure, including cellular stress response mechanisms, such as molecular chaperone synthesis and apoptosis. Tissue remodeling processes were also identified as transient, but took place later in the timeline, suggesting their importance to long-term acclimation as they likely equip the fish with lasting adaptations to their new environment. The alterations in branchial functional pathways displayed by Arabian pupfish in response to salinity increases are diverse. These reveal a large toolkit of molecular processes important for adaptation to hyperosmolarity that allow for successful colonization to a wide variety of different habitats.

Introduction

Salinity is one of the main abiotic factors shaping the distribution and habitat preference of fish and other aquatic taxa. Teleosts have evolved different strategies to maintain osmotic homeostasis depending on water ion concentrations. In seawater, fish drink copiously to combat water lost via osmosis, concurrently suffering passive intake of high quantities of salts. Specialized mitochondria-rich cells of the gill epithelium, called ionocytes, are then responsible for active excess ion secretion (Edwards & Marshall, 2012; D. H. Evans, Piermarini, & Choe, 2005). In freshwater, fish face ion loss and passive osmotic water intake. To compensate for the consequent dilution of their body fluids, they actively uptake ions from the surrounding medium through specialized ionocytes (Edwards & Marshall, 2012; D. H. Evans et al., 2005). Given the profound differences in osmoregulatory mechanisms in fresh versus seawater, changes in salinity represent a significant challenge for fish, and the induced osmotic stress can lead to interferences with physiological homeostasis and impairment of biological processes (Kultz, 2015). As a consequence, most teleost fishes are restricted to limited habitat salinities (stenohaline fish). Other species, termed euryhaline fish, have evolved osmoregulatory plasticity in the organs involved in maintenance of osmotic balance (Schultz & McCormick, 2012). In particular plastic modifications to the gill epithelium, the main tissue responsible for osmoregulation in fish (D. H. Evans et al., 2005), grant the ability to live in wider salinity ranges and exploit larger habitat diversity.

Extensive work has been performed to understand the molecular underpinnings responsible for gill plasticity in euryhaline species. Early studies focused on salinity-driven expression changes of specific ion transporters and osmoregulatory genes (Deane & Woo, 2004; Scott, Claiborne, Edwards, Schulte, & Wood, 2005; Scott, Richards, Forbush, Isenring, & Schulte, 2004), expanding the existing knowledge regarding branchial ion secretion and absorption mechanisms. In particular, the role of Na^+/K^+-ATPase (NKA), $Na^+/K^+/Cl^-$ transporter

(NKCC1), and cystic fibrosis transmembrane conductance regulator (CFTR) in marine-type ion-extruder ionocytes was extensively investigated, and found to be highly conserved in seawater adapted teleosts (Edwards & Marshall, 2012; D. H. Evans et al., 2005). In contrast, the mechanisms for ion absorption were found to be quite diverse across different species, and several ionocytes subtypes have been described in freshwater adapted fishes (Dymowska, Hwang, & Goss, 2012; Hiroi & McCormick, 2012; Hsu, Lin, Tseng, Horng, & Hwang, 2014; Hwang & Lin, 2013). Advancements in molecular and sequencing technologies have led to the discovery of additional essential pathways for osmoregulation in euryhaline fish. Transcriptomics has provided the means to identify genes and pathways involved in osmosensing and activation of signalling cascades that initiate the osmotic stress response and the acclimation processes (T. G. Evans & Somero, 2008; Fiol & Kultz, 2007; Komoroske et al., 2016; Kultz, 2012). Profound gill remodelling, observed by microscopy and immunocytochemistry studies as alterations in ionocyte morphology and abundance (Foskett, Logsdon, Turner, Machen, & Bern, 1981; Katoh & Kaneko, 2003; Uchida, Kaneko, Miyazaki, Hasegawa, & Hirano, 2000), was linked to salinity-specific ion transporter and protein *de novo* synthesis or relocation inside the cell, activation of apoptosis pathways, and modifications of the cytoskeleton, cell-cell junctions, and the extracellular matrix (Jeffries et al., 2019; Lam et al., 2014; Mundy, Jeffries, Fangue, & Connon, 2020; Whitehead, Roach, Zhang, & Galvez, 2012). Euryhaline fish are therefore able to switch between hypo- and hyper-osmoregulation when confronted with changes in environmental salinity, although rapid increases in intra- and extra-cellular ion concentrations can negatively affect structural and functional properties of tissue macromolecules, such as proteins, lipids and DNA (Burg, Ferraris, & Dmitrieva, 2007; T. G. Evans & Kultz, 2020). Markers for an evolutionary conserved cellular stress response (CSR) triggered by macromolecular damages have been identified in gene expression and transcriptomic studies in fish exposed to changes in salinity (Brennan, Galvez, & Whitehead,

2015; Tine, Bonhomme, McKenzie, & Durand, 2010; Whitehead, Zhang, Roach, & Galvez, 2013). The CSR is comprised of defence mechanisms to protect cellular components, including the expression of molecular chaperones, and to re-establish homeostasis, by accumulation of organic compatible osmolytes and osmoregulatory mechanism switch. Moreover, the replication of damaged DNA is prevented through transcription inhibition, apoptosis and cell cycle arrest (Burg et al., 2007; T. G. Evans & Kultz, 2020; Kultz, 2005). The processes of osmotic stress response, ion homeostasis restoration and tissue remodelling are energetically demanding for euryhaline fish (T. G. Evans & Kultz, 2020; Takei & Hwang, 2016; Tseng & Hwang, 2008), and differential regulation of metabolic and mitochondrial respiration pathways during salinity challenges have been reported in several studies (Brennan et al., 2015; Chen, Lui, Ip, & Lam, 2018; T. G. Evans & Somero, 2008; Nguyen, Jung, Nguyen, Hurwood, & Mather, 2016). Given the large percentages of their energy budget consumption in response to osmotic stress, compromises in the allocation of energetic resources have been hypothesized, and consequent impairments in physiological processes such as development, growth and immune response have been reported (Bœuf & Payan, 2001; Komoroske et al., 2016; Makrinos & Bowden, 2016; Morgan & Iwama, 1991). While a variety of processes involved in osmotic stress and salinity acclimation in teleosts have been defined, their ecological adaptive potential in natural colonization events is still not clear, especially the exact timing of stress, acclimation and adaptation responses and mechanisms. A number of time series salinity acclimation studies have been performed (Brennan et al., 2015; T. G. Evans & Somero, 2008; Komoroske et al., 2016; Kozak, Brennan, Berdan, Fuller, & Whitehead, 2014; Scott et al., 2004; Whitehead, Roach, Zhang, & Galvez, 2011), using designated single gene or microarray expression analyses. However, RNAseq whole-genome transcriptomics combined with an appropriate model species and collection time point selection would allow for the capture of a more

119 complete picture of both the temporal and the mechanistic aspects of the branchial salinity
120 response in euryhaline fish during highly saline habitat colonization.

121 The Arabian pupfish, *Aphanius dispar* (Rüppell, 1829), is a euryhaline species member of the
122 Cyprinodontidae family with widespread habitat ranges (Hrbek & Meyer, 2003). Its
123 distribution encompasses areas around the Red Sea, the Persian Gulf, the Arabian Sea, and part
124 of the south-eastern Mediterranean basin, with populations living from inland freshwater
125 reservoirs to coastal lagoons, and hot sulphuric springs. Along the western coast of Saudi
126 Arabia, the Arabian pupfish is found in a large variety of environmental salinities, ranging from
127 highly saline (41 – 44 ppt) Red Sea coastal lagoons to nearly-freshwater desert oases (0.7 – 1.5
128 ppt) with no permanent connection to the sea. While salinity changes have been observed to
129 influence Arabian pupfish osmotic pressure, body ion content, and gill permeability (Lotan,
130 1969, 1971), no differences in performance indicators, such as resting metabolic rate,
131 swimming speed and activity level, were caused by up to 70 ppt increases in water salinity
132 (Plaut, 2000). In a recent genetic connectivity study supported by hydrological mapping of the
133 region, the coastal Red Sea populations have been found to receive migrants from the inland
134 ponds as a result of sporadic flash flood events that wash individuals out to the sea (Schunter
135 et al., 2021). These colonization events require considerable acclimation capacities in order to
136 survive such a rapid and drastic change in environment, especially while coping with the abrupt
137 increase in salinity. For these reasons, the Arabian pupfish represents an excellent system to
138 investigate the mechanisms underlying the plasticity of euryhaline fish gills during salt stress
139 events, and the processes that allow them to acclimate long-term and colonize novel habitats.
140 In this study, nearly-freshwater adapted Arabian pupfish from inland desert ponds were
141 transferred to highly saline water to mimic a colonization event. The acclimation course was
142 explored over time to disentangle the short-term processes responding to acute osmotic stress

143 from the strategies providing the fish with longer-term adjustments required for prolonged
144 adaptation in seawater environments.

145

146 **Materials and methods**

147 *Experimental design*

148 To evaluate the natural acclimation of Arabian pupfish from near-freshwater to a large increase
149 in salinity over a short period of time, adult *Aphanius dispar* from the same genetic unit
150 (Schunter et al., 2021) were collected using a seine net from two Saudi Arabian sites, including
151 a near-freshwater (1.45 ppt) desert pond and a highly saline Red Sea coastal lagoon (43.49
152 ppm; Suppl. Table 1) between November 2015 and January 2016 (Fig. 1).

153

154 The fish were transported to the King Abdullah University of Science and Technology Coastal
155 and Marine Resources Core Lab and maintained in closed-system tanks to habituate to holding
156 conditions for at least eight months prior to experiments. The conditions in the aquaria
157 resembled those of the collection sites with 26°C water temperature, 8.32 ± 0.03 pH, 10L:14D
158 photoperiod, and salinity at 1.92 ppt ± 0.01 SE for the desert pond fish and 42.68 ppt ± 0.09
159 SE for the coastal lagoon fish (Suppl. Table 2). Salinity was achieved using seawater, diluted
160 for the desert pond fish with dechlorinated tap water. All fish were kept at maximum densities
161 of seven individuals per tank, in six replicate tanks per treatment, and fed once a day *ad libitum*
162 with commercial pelleted feed. In October 2016, the osmotic challenge experiment started: fish
163 from the desert pond population were directly transferred to seawater, in order to mimic the
164 change in salinity experienced during colonization of coastal lagoons of the Red Sea (Fig. 2).
165 Temperature, photoperiod and pH were kept constant during the entire duration of the
166 experiment in order to avoid any confounding effects. Fish were sampled pretransfer (0 h) from

both populations (1.9 ppt and 43 ppt), and at five post-transfer time points (43 ppt; 6 h, 24 h, 72 h, 7 days, 21 days). At each sampling event, six individuals (one per different replicate tank) were rapidly euthanized using an overdose of tricaine methanesulphonate (MS-222, MP Biomedicals), sexed, and length was measured (Suppl. Table 3). For each individual, the right gill basket was excised and snap-frozen in liquid nitrogen and stored at -80°C for subsequent RNA extraction.

RNA-sequencing and transcriptome assembly

RNA was isolated from gill samples using a Qiagen AllPrep DNA/RNA mini kit, following homogenization in RLT Plus buffer with MP Biomedicals FastPrep-24 homogenizer, and DNase I treated (RNase-Free DNase Set, Qiagen). Sample quality was checked using a TapeStation RNA ScreenTape assay (Agilent). Samples that did not meet RNA quality/quantity standards were excluded from the analysis. Libraries for paired-end fragments were prepared from a total of 33 samples (3-6 sample/time point) using the Illumina TruSeq stranded mRNA Library Preparation Kit, according to the manufacturer's protocol, with each sample uniquely barcoded. Quality control check and quantification were performed with a Bioanalyzer High Sensitivity DNA assay (Agilent). Three library pools were run on an Illumina HiSeq 4000 by the King Abdullah University of Science and Technology Bioscience Core Lab.

Raw reads were processed for quality trimming and adapter removal with Trimmomatic v0.36 (Bolger, Lohse, & Usadel, 2014), using ILLUMINACLIP:2:30:10 HEADCROP:10 SLIDINGWINDOW:4:20 MINLEN:70, and inspected with FastQC (Andrews, 2010) before and after quality filtering. Trimmed reads were later corrected from random sequencing errors using a *k*-mer based method, Rcorrector (Song & Florea, 2015). Unfixable reads were discarded. Trimmed and corrected reads from all samples were used to *de novo* assemble the

191 *A. dispar* gill transcriptome using Trinity v2.4.0 (Grabherr et al., 2011) with default settings.
192 The assembly was then decontaminated using a hierarchical clustering algorithm called Model-
193 based Categorical Sequence Clustering (MCSC; Lafond-Lapalme, Duceppe, Wang, Moffett,
194 & Mimee, 2017). The MCSC pipeline was tested at five different clustering levels to determine
195 the best one (level 3, based on the highest SS ratio), and the superclass Actinopterygii was
196 chosen for the white list ratio calculation. Putative coding regions were predicted by
197 TransDecoder v5.5.0 (Haas et al., 2013), and integrated with homology search against the Pfam
198 protein domain database using HMMER v3.2.1 (Finn, Clements, & Eddy, 2011), and the
199 UniRef90 protein database using blastp (BLAST+ v2.6.0; Camacho et al., 2009), evalue $\leq 1e^{-5}$.
200 The decontaminated assembly was then filtered based on TransDecoder results, retaining
201 only the single best open reading frame (ORF) per transcript. Sequence redundancy was
202 reduced using cd-hit-est from the CD-HIT v4.8.1 package (Fu, Niu, Zhu, Wu, & Li, 2012) with
203 95% identity as clustering threshold. At each filtering stage, the quality of the assembly was
204 evaluated by checking the basic alignment summary metrics, as well as quantifying the read
205 representation by mapping the cleaned reads back to the transcriptome with Bowtie2 v2.3.4.1
206 (Langmead & Salzberg, 2012). Moreover, to evaluate the completeness of the assembly, and
207 to control for potential loss of core genes during the filtering process, BUSCO v3.02 (Simao,
208 Waterhouse, Ioannidis, Kriventseva, & Zdobnov, 2015) was run after every filtering step, using
209 the provided Actinopterygii set of 4,584 Benchmarking Universal Single-Copy Orthologs.

210

211 *Annotation, differential gene expression and gene ontology analysis*

212 Transcriptome annotation was performed first by BLAST searches of the TransDecoder
213 predicted ORFs and the untranslated transcripts, using blastp and blastx algorithms respectively
214 (evalue $\leq 1e^{-5}$), against the UniProtKb and the NCBI non-redundant (nr) databases. Where
215 conflicts were found, the following order of priority was observed: UniProtKb/Swiss-Prot,

NCBI nr, and UniProtKb/TrEMBL. BLAST results were then loaded in OmicsBox v1.4.11 (BioBam Bioinformatics, 2019), where Gene Ontology (GO), InterPro, and EggNOG (Huerta-Cepas et al., 2019) annotations were additionally performed using Blast2GO (Gotz et al., 2008).

To test for gene differential expression between the two source populations, as well as along the salinity acclimation time series, reads from each sample were first quantified using Salmon v1.1.0 (Patro, Duggal, Love, Irizarry, & Kingsford, 2017) in mapping-based mode against the *de novo* assembled transcriptome. Transcript abundance estimates were then summarized at gene level and imported in DESeq2 v1.26.0 (Love, Huber, & Anders, 2014) using the package tximport v1.14.2 (Soneson, Love, & Robinson, 2015) in R v3.6.1. Principal component analyses were run to visually check for possible overall patterns, outliers and batch effects. Three samples (DP_Rep1, T2_Rep4, T5_Rep5) were labelled as outliers and excluded from the DE analysis. Differentially expressed genes (DEGs) were identified running pairwise comparisons of control populations and post-transfer time points using the *contrast* function of DESeq2 with shrunken log2 Fold Change (log2FC) estimates by apeglm (Zhu, Ibrahim, & Love, 2019). $|\text{Log2FC}| \geq 0.3$, False Discovery Rate (FDR) adjusted *p*-value (Benjamini & Hochberg, 1995) < 0.05 (Wald test), and a mean expression of > 10 reads (baseMean) were used as thresholds.

To identify groups of genes showing comparable trends, such as rapid or longer-term responses to the salinity challenge, DEGs revealing similar expression patterns across time points were clustered. Additionally, ImpulseDE2 v1.10.0 (Fischer, Theis, & Yosef, 2018), a Bioconductor R package specifically designed for time series data, was employed in case-only mode to

discern steadily increasing or decreasing expression trajectories from transiently up- or down-regulated genes. For all clustering purposes, Red Sea population samples were treated as if they belonged to an additional time-point, the last in the acclimation timeline (long-term acclimation beyond three weeks).

Functional enrichment analyses were performed in OmicsBox v1.4.11 (BioBam Bioinformatics, 2019), with the Fisher's Exact Test (FDR < 0.05) after removing duplicated annotations from the differentially expressed genes (DEGs) and identified gene cluster sets to find over-represented GO terms between controls and post-transfer time points.

Results

Transcriptome assembly and annotation

The first *de novo* transcriptome assembly for *Aphanius dispar* was created from a total of 1.38 billion raw reads with an average of 24.5 million reads per sample after trimming and error correction steps (Suppl. Table 3). These high-quality reads were used to *de novo* assemble the Arabian pupfish gill transcriptome, which resulted in 650,824 contigs with a 97.2% overall mapping rate, an N50 of 1,275 bp, and 86.2% BUSCO completeness score using the Actinopterygii database (Suppl. Table 4). A total of 2.9% contigs were filtered out in the decontamination step, and among the remaining 631,806, 141,428 contigs were predicted to contain a coding region. The final redundancy reduced transcriptome resulted in 99,167 contigs of N50 2,302 bp, E90N50 2,519 bp, with an average of 75.0% mapping rate and 86.1% of complete BUSCO genes. Tximport gene-level summarization of the final transcriptome yielded 55,451 genes. 36,863 of these genes (66.5%) were successfully annotated using SwissProt database, and another 11,078 genes had hits in the NCBI nr database. 446 more

genes had positive blast hits when searched against TrEMBL, for a combined total of 48,337 annotated genes (87.2%).

Gene expression differences in natural populations

The two sampled populations, desert pond (DP) and the highly saline Red Sea (RS) coastal lagoon, exhibited a clear branchial gene expression separation (time 0; Fig. 3), which was partly conserved throughout the salinity challenge (Suppl. Fig. 1). The pairwise comparison of fish in their original salinities resulted in 552 differentially expressed genes (DEGs; Suppl. Table 5) which is the second largest expression difference of the experiment (Fig. 4). Several functions were differentially regulated in the two populations, in particular ion transport and immune system.

Ion transport related terms represented 70% of total enriched GO categories between the populations at time 0 (Suppl. Table 6). The RS individuals in particular upregulated specific seawater ion transporters, such as the $Na^+/K^+/Cl^-$ transporter (SLC12A2), the cystic fibrosis transmembrane conductance regulator (CFTR), and the transient receptor potential (TRP) cation channel subfamily V member 1 (TRPV1), together with genes involved in their regulation, such as serine/threonine kinase 39 (STK39) and the WNK lysine deficient protein kinase 2 (WNK2). Similarly upregulated in the RS population were other ion transporters and genes important in osmoregulation such as potassium channels and their modulators (KCNN3, KCNJ1, KCNJ15, ABCC8), voltage-gated calcium channel subunits (CACNA1H, CACNA1S), ammonium transporters Rh (RHAG, RHCG), sodium/hydrogen exchangers and regulators (NHEB, SLC9A2, SLC9A3R2), as well as inositol monophosphatase 1 (IMPA1) and vasoactive intestinal peptide (VIPR1). Several Na^+/K^+-transporting ATPase subunits (ATP1A1, ATP1A3) were also differentially expressed between the two populations, and

288 elevated expression in the nearly-freshwater DP fish was found for a different set of ion
289 channels, including members of the transient receptor potential (TRP) cation channel
290 superfamily (TRPM2, TRPM5, TRPM7, TRPV4), chloride channels like the chloride channel
291 protein 2 (CLCN2), the inward rectifier potassium channel 2 (KCNJ2), and the intracellular
292 channel inositol 1,4,5-trisphosphate receptor type 1 (ITPR1), together with its modulator, the
293 calcium binding protein 1 (CABP1). Aquaporin 3 (AQP3) was also upregulated in DP samples.

294 The two populations also showed differential regulation of the immune system. C-C motif
295 chemokine ligands 3 and 25 (CCL3, CCL25) were upregulated in the RS population, while
296 members of the C-X-C motif chemokine family (CXCL8, CXCL11.6, CXCL14) were
297 upregulated in the DP fish, enriching the "chemokine activity" function. Moreover, C-C
298 chemokine receptors (CCR4, CCR6) were upregulated in the gills of the DP population, while
299 several genes coding for components of acquired immunity were upregulated in the seawater
300 RS individuals, like immunoglobulins and major histocompatibility complex proteins (IGKC,
301 IGHM, IGL1, IGKV4-1, MR1, H2-EA).

302 A few other functions were divergent between the populations, such as polyamine metabolism,
303 whose related genes (ODC1, ARG1, PAOX) were upregulated in DP. Two functions were
304 exclusive to the RS population: O-linked glycosylation, represented by five upregulated genes
305 (B3GNT7, ST3GAL1, STR3GAL2, ST6GALNAC2, ST8SIA6), and keratinization, with the
306 upregulation of cornifelin (CNFN), envoplakin (EVPL), keratins (XK70A, K1C1), and
307 transglutaminase 5 (TGM5).

308

309 *Time course of the molecular responses to the salinity challenge*

310 The selected experimental timeline and the clustering analyses of differentially expressed genes
311 along the acclimation window (Fig. 4) allowed for the discovery of distinctively timed

312 processes in the Arabian pupfish branchial response to the abrupt increase in salinity. While
313 some DEGs were only transiently differentially regulated along the acclimation timeline (Fig.
314 5a), 231 and 269 genes steadily increased or decreased, respectively (Fig. 5b; Suppl. Table 7),
315 and in particular the downregulated genes exhibited enrichment in cell cycle related terms
316 (Suppl. Table 8). Through the investigation of each time point, mechanisms typical of a short-
317 term stress response were uncovered at 6 and 24 h post-transfer, while the 72 h and 7 day time
318 points revealed cell cycle arrest and tissue remodelling events, and the last time point (21 day
319 post-transfer) was characterized by longer-term acclimation processes, many resembling the
320 Red Sea population transcriptional profile (Fig. 6).

321

322 Just six hours after the start of the hyperosmotic challenge, 75 branchial genes showed a
323 statistically significant change in expression compared to pre-transfer controls (Suppl. Table
324 9). This immediate reaction was based on a wide array of different functions (Suppl. Table 10).
325 The acute osmotic stress caused the onset of cell signalling cascades, with the differential
326 expression of prolactin receptor (PRLR), the stress responsive hydroxysteroid 11-beta
327 dehydrogenase 2 (HSD11B2), which modulates intracellular cortisol levels, and
328 serum/glucocorticoid regulated kinase 1 (SGK1), important in the cellular stress and DNA
329 damage responses. Furthermore, the osmotic stress response was found to entail ion
330 homeostasis pathways, through the regulation of ion transport and ion channel activity (CFTR,
331 KCNJ2, TCAF, WNK2), and organic osmolyte synthesis and transport (GLUL, IMPA1,
332 ISYNA1-B, SLC6A20, SLC5A7, ABCG20). In particular, ISYNA1-B was transiently
333 upregulated between 6 and 24 hours and, in the same interval, IMPA1 showed very high levels
334 of expression, while being upregulated across the whole timeline (Suppl. Fig. 2a). Another
335 important function found at 6 hours post-transfer was tissue modification, by means of cellular
336 proliferation and differentiation (GPM6B, NR4A3, NHSL1), and keratinization (CNFN,

337 DSC1). Genes involved in the immune response were also differentially expressed at 6 hours,
338 and class I histocompatibility antigen, F10 alpha chain (HA1F) was upregulated post-transfer.
339 Upregulation of genes implicated in lipid (ALOXE3, ALOX15B, CPT1A) and glucose (GAD1,
340 SLC2A8) metabolism and transport was also found. Although a few DEGs were found to be
341 related to circadian rhythm processes (NFIL3, NR1D1, NR1D2, PER2), this result is most
342 likely due to the sampling time occurring at a different moment of the day, rather than an effect
343 of the salinity change.

344

345 At 24 h post-transfer, there were 164 DEGs compared to time 0 (Suppl. Table 11). "Gland
346 development" was among the enriched GO terms (Suppl. Table 12), and included genes related
347 to secretion, such as sodium and chloride channels (CFTR, CLCN2, SLC12A2), cell
348 proliferation (E2F7, FGF7, FOXM1), hormonal response to stress actors (CRHR1, PRLR),
349 cytoskeleton and extra-cellular matrix organization genes (DIAPH3, SOX9). "Lipid metabolic
350 process" was also enriched at 24 hours, with genes related to cell membrane glycosphingolipid
351 and glycerophospholipid biosynthesis (B4GALNT1, PLAAT4) and genes involved in lipid
352 transport, such as carnitine palmitoyltransferase 1A (CPT1A), known to be part of the
353 mitochondrial fatty acid oxidation pathway, and already upregulated at 6 hours. The increased
354 energetic demand was additionally manifested by the upregulation of NADH:ubiquinone
355 oxidoreductase complex assembly factor 4 (NDUFAF4), and solute carrier family 24 member
356 48 (SLC25A48), among others. Several ion transport actors and osmotic stress response
357 regulators still played a role at 24 hours as did various transcription factors, repressors, and
358 regulators (Suppl. Table 10). Some genes involved in DNA damage response pathway also still
359 showed differential expression. Noteworthy, several genes involved in keratinization (CNFN,
360 K1C1, KRT13, S100A11, TGM5) were upregulated compared to time 0, while there was a
361 downregulation of genes involved in the extracellular matrix degradation (ADAMTS5,

362 COL23A1, EFEMP2, PLOD2, THSD4). Tissue remodelling processes happening in
363 transferred fish were additionally reflected by the differential expression of genes involved in
364 the regulation of apoptosis (Suppl. Table 10), such as cytochrome C (CYC), solute carrier
365 family 25 member 6 (SLC25A6) and voltage-dependent anion channel 2 (VDAC2), all thought
366 to be involved in the mitochondrial apoptotic pathway.

367

368 Clustering revealed that most of the above-mentioned genes exhibited a transiently up- or
369 down-regulated pattern in the first 24 hours, being differentially expressed compared to pre-
370 transfer fish only in these early time points (Fig. 5a; Suppl. Fig. 2; Suppl. Table 13). The main
371 differences between the 6 and 24 h post-transfer time points (109 DEGs; Suppl. Table 14), as
372 portrayed by the many related enriched GO terms (Suppl. Table 15), lay in cell cycle and
373 mitosis associated processes, with downregulation of over 30 genes with these functions at 24
374 hours.

375

376 Individuals from the 72 hour time point compared with the 24 h post-transfer fish resulted in
377 only 30 DEGs (Suppl. Table 16), including the downregulation of two heat shock protein
378 coding genes (HSPE1, DNAJC15) involved in stress response. The comparison with fish pre-
379 transfer identified 197 DEGs (Suppl. Table 17), and the strongest signal of this contrast was
380 the downregulation of more than 30 genes (Suppl. Table 10) involved in mitotic cell cycle and
381 cell population proliferation (Suppl. Table 18), such for example genes fundamental for G1/S
382 and G2/M phase transitions of the cell cycle. Concurrently, genes involved in DNA replication
383 and repair showed downregulation compared to time 0 (Suppl. Table 10). Branchial tissue
384 modifications were still happening at 72 hours with DEGs involved in extracellular matrix
385 degradation including: Ca^{2+}-activated cysteine protease calpains (CAPN2, CAPN5, CAPN8),

386 and matrix metallopeptidase 8 (MMP8), known to play a role in the breakdown of the
387 extracellular matrix during tissue remodelling, as well as several glycoproteins with cell
388 adhesion functions, such as CEA cell adhesion molecules (CEACAM5, CEACAM6). Genes
389 belonging to the glycosaminoglycan - or mucopolysaccharides - biosynthesis pathway were
390 upregulated at 72 hours compared to pre-transfer conditions (Suppl. Table 10).

391

392 After 7 days from the start of the hyperosmotic challenge there were 423 DEGs compared to
393 pre-transfer fish at time 0 (Fig. 4; Suppl. Table 19). This observed high number of differentially
394 expressed genes could be an effect of the small sample size for this time-point (n = 3).
395 Numerous GO terms were enriched (Suppl. Table 20), and over 80 genes, mostly
396 downregulated compared to time 0, pertained to mitotic cell cycle as well as cell proliferation
397 and differentiation processes (Suppl. Table 10). Seven-day post-transfer fish gills were still
398 showing significant changes in the expression of several ion channels, as well as genes
399 implicated in energy production and tissue modifications, such as cell adhesion, cytoskeleton
400 organization, mucopolysaccharide metabolism, and extracellular matrix degradation (Suppl.
401 Table 10).

402

403 The last time point at 21 days post transfer exhibited 139 DEGs (Suppl. Table 21) in
404 comparison with pre-transfer fish. There was no functional enrichment for these genes, which
405 were involved in a variety of processes (Suppl. Table 10). Osmoregulation was still under
406 transition, with the upregulation of two typical seawater sodium-coupled transporters, the
407 ATPase Na^+/K^+ transporting subunit alpha 1 (ATP1A1) and the solute carrier family 12
408 member 2 (SLC12A2). While cell cycle and energy production genes were not differentially
409 expressed at 21 days, gene expression related genes and tissue organization were upregulated

compared to time 0 (Suppl. Table 10). Moreover, two genes involved in the biosynthesis of mucopolysaccharides (GALT-1, ST3GAL1) showed upregulation, joining B3GNT7, CHST3, ST3GAL2 that were already upregulated earlier in the acclimation.

Expression signatures leading to adaptation

Additional clustering analyses focused on the identification of genes putatively critical to long-term acclimation to elevated salinity in the Arabian pupfish. Starting from a subset of genes differentially expressed between the two populations at time 0, the focus was placed on 69 DEGs that along the experimental timeline progressively resembled the expression levels of the Red Sea population (Suppl. Table 22). Overall, some functions appeared earlier than others along the acclimation window (Fig. 6). For example, many genes implicated in osmotic stress response and osmoregulation (CA4, CFTR, CLCN2, IMPA1, KCNJ1, STK39, USP2, WNK2) were among the first to steadily change expression, between 6 and 24 hours from the start of the exposure. Cornifelin (CNFN), a component of the cornified cell envelope, and glycoprotein M6B (GPM6B), a key upstream regulator of genes involved in actin cytoskeleton organization, were upregulated at every time point post-transfer. Similarly, genes involved in the metabolism of polyamines (ODC1, PAOX), important in hyposaline acclimation in teleosts, were downregulated from the first 24 hours of exposure. As time progressed more genes changed their expression to match that of the seawater population. At 72 h post-transfer, the functions of these genes were related to changes in tissue organization and permeability, with the upregulation of calpain 2 (CAPN2) and microfibril associated protein 4 (MFAP4), both part of the extracellular matrix degradation pathway, and the downregulation of the water channel aquaporin 3 (AQP3). Moreover, some genes involved in mucopolysaccharide metabolism (B3GNT7, CHST3, GALT-1) started to be upregulated at 72 hours, while others (ST3GAL1, ST3GAL2) showed upregulation after 7 days. From 7 days of exposure to sea water, the

435 transferred fish started to change the expression of branchial genes involved in lipid
436 metabolism, showing upregulation of neutral cholesterol ester hydrolase 1 (NCEH1) and
437 downregulation of low-density lipoprotein receptor (LDLR), both involved in lipoprotein and
438 cholesterol metabolism. The transient receptor potential cation channel subfamily V member
439 4 (TRPV4), a non-selective cation channel involved in osmotic pressure regulation, was also
440 downregulated from 7 day post-transfer. Finally, at the end of the experimental acclimation
441 period, 21 days post-transfer, there was a downregulation of glycine decarboxylase (GLDC),
442 involved in osmotic regulation, and arginase 1 (ARG1), another component of the polyamine
443 metabolism pathway.

444

445 **Discussion**

446 Arabian pupfish from nearly-freshwater ponds (1.5 ppt) are sporadically being flushed out to
447 highly saline environments of the Red Sea (43 ppt) through dry riverbeds (called "wadies") by
448 flash floods (Schunter et al., 2021), where they are able to rapidly acclimate to the new
449 environment and establish viable populations. Comparing the gill gene expression profiles of
450 the native populations, as well as the changes across a salinity challenge from hours to weeks
451 post-transfer, enabled the separation between short- and longer-term osmotic stress responses,
452 and the investigation of the processes that allow pupfish to adapt to the high salinity typical of
453 the Red Sea environment. The native nearly-freshwater pupfish were able to acclimate to the
454 abrupt increase in water salinity by means of expression changes in a large number of branchial
455 genes. A subset of genes whose expression changed with the salinity exposure to resemble
456 those of native seawater individuals revealed the importance of related functions in long-term
457 acclimation.

458

Osmoregulation was the primary function at play during pupfish acclimation to high salinity, as well as the main source of expression divergence between the two native populations. When in seawater, teleosts need to extrude passively accumulated salts through a variety of branchial ion transporters (D. H. Evans et al., 2005). Accordingly, the Arabian pupfish Red Sea population upregulated ion transporters and osmoregulation related genes typically found in marine teleosts (Hiroi & McCormick, 2012; Hwang, Lee, & Lin, 2011). The expression of many of these genes was quickly upregulated following high salinity exposure in desert pond fish and maintained along the entire acclimation timeline. For instance, genes involved in chloride ion secretion in marine-type ionocytes, such as cystic fibrosis transmembrane conductance regulator (CFTR) and $Na^+/K^+/Cl^-$ transporter (NKCC1 or SLC12A2; Hiroi & McCormick, 2012; Marshall, 2011), were upregulated in transferred pupfish already from 6 and 24 hours, respectively. Accordingly, in another pupfish species, *Cyprinodon nevadensis amargosae*, CFTR and NKCC1 gill mRNA levels increased within a similar time frame post-transfer into seawater and remained elevated throughout the two week experiment (Lema, Carvalho, Egelston, Kelly, & McCormick, 2018), and upregulation of these two genes was also found in the gills of mummichog (*Fundulus heteroclitus*) within 24 h post-transfer from brackish to seawater (Scott et al., 2004). Involved in the activation of NKCC1 are two other genes, WNK lysine deficient protein kinase 2 (WNK2) and serine/threonine kinase 39 (STK39) (Delpire & Gagnon, 2008; Flemmer et al., 2010; Marshall, 2011), also differentially expressed across the timeline in Arabian pupfish. WNK2 has indeed been found to regulate NKCC1 activation in *Xenopus* oocytes (Rinehart et al., 2011), and its upregulation at every time point post-transfer to hyperosmotic water was also reported in the gills of the butterfish *Pampus argenteus* (Li et al., 2020). Likewise, Flemmer et al. (2010) reported the upregulation of STK39 in seawater-acclimated mummichog gills, and additionally linked it to the increased expression of NKCC1 in the same samples. The prompt upregulation of marine-type ion transporters and

484 osmoregulatory genes in desert pond pupfish exposed to seawater to quickly resemble the Red
485 Sea population levels confirms the importance of these genes in osmoregulation to highly saline
486 conditions and reveals the high degree of conservation in osmoregulatory mechanisms among
487 different fish species, Arabian pupfish included.
488
489 Another fundamental component of teleost osmoregulation in salt water is the *myo*-inositol
490 biosynthesis (MIB) pathway, through which the compatible organic osmolyte *myo*-inositol is
491 synthetized and accumulated inside cells during osmotic stress for protection from salinity-
492 induced damages (Yancey, Clark, Hand, Bowlus, & Somero, 1982). The two enzymes
493 constituting the MIB pathway, inositol monophosphatase 1 (IMPA1) and *myo*-inositol
494 phosphate synthase (MIPS or ISYNA1), were both differentially expressed in high-salinity
495 exposed pupfish. Accordingly, both genes were also upregulated following seawater transfer
496 in other euryhaline fishes, such as eels (*Anguilla anguilla*; Kalujnaia, McVee, Kasciukovic,
497 Stewart, & Cramb, 2010) and turbots (*Scophthalmus maximus*; Cui et al., 2020), where the
498 MIB pathway knockdown was directly implicated in causing weakened gill osmoregulation
499 and reduced survival (Ma et al., 2020). The MIB pathway is therefore an important
500 osmoregulation mechanism in seawater across several different species. However, the transient
501 upregulation of MIPS in the first 24 hours only highlights the importance of this pathway in
502 the short-term osmotic stress response of the Arabian Pupfish.
503
504 In hyposaline waters fish are susceptible to passive ion loss and need to compensate by active
505 uptake of osmolytes from the surrounding water (Edwards & Marshall, 2012). In Arabian
506 pupfish, chloride uptake is likely accomplished by chloride ion channel protein 2 (CLCN2),
507 typically found in freshwater ionocytes (Leguen, Le Cam, Montfort, Peron, & Fautrel, 2015;
508 Wang, Yan, Tseng, Chen, & Hwang, 2015), which was highly expressed in desert pond

509 individuals pre-transfer, and decreased from 24 hours of high salinity exposure onward.
510 Rainbow trout (*Oncorhynchus mykiss)* ionocytes (Leguen et al., 2015) and a Sacramento
511 splittail population exposed to seawater *(Pogonichthys macrolepidotus*; Mundy et al., 2020)
512 also show this pattern, indicating the importance of this chloride channel in a variety of fish
513 species inhabiting freshwater environments, where chloride uptake from the surrounding water
514 is a key aspect of osmoregulation. Conversely, desert pond Arabian pupfish lack most of the
515 previously described mechanisms for the uptake of sodium (Dymowska et al., 2012; Hsu et al.,
516 2014), and might possibly exclusively rely on specialized isoforms of Na^+/K^+-ATPase (NKA)
517 subunits for its import. Although the NKA gene is usually identified in marine acclimated
518 teleosts, where it is part of the ion secretion machinery, in Arabian pupfish different transcripts
519 annotated to the α-1 subunit gene were upregulated in desert pond individuals, and only one
520 transcript was upregulated in Red Sea pupfish. While this could be an indication of population-
521 specific NKA subunit α-1 isoforms (Mundy et al., 2020), it is likely that salinity-dependent
522 isoforms with opposite functions of ion uptake in hyposaline water and salt secretion in
523 seawater exist in this species, as previously described for several euryhaline teleosts
524 (Bystriansky, Richards, Schulte, & Ballantyne, 2006; McCormick, Regish, & Christensen,
525 2009; Richards, Semple, Bystriansky, & Schulte, 2003; Tipsmark et al., 2011; Urbina, Schulte,
526 Bystriansky, & Glover, 2013; Velotta et al., 2017). In the climbing perch (*Anabas testudines*)
527 and in salmonids, NKA α-1 isoform a expression levels are highest in freshwater and decreases
528 post-transfer to seawater, while other isoform mRNA expressions increase following exposure
529 (Bystriansky et al., 2006; Ip et al., 2012). Accordingly, some of the NKA α-1 subunit coding
530 transcripts showed a steady decreasing pattern along the exposure timeline in transferred
531 pupfish, with one transcript resulting in a 4.5-fold downregulation at the end of the
532 experimental timeline, which could be an indication of acclimation to the seawater habitat,
533 where sodium uptake is not needed anymore. Revealed Arabian pupfish hyperosmoregulatory

534 mechanisms could represent a new model for fish branchial ion absorption at low salinities and
535 confirm the wide diversity of evolutionary distinct branchial adaptations to hyposaline
536 environments in teleosts. Overall, the main mechanisms differentiating Arabian pupfish natural
537 populations pertain to osmoregulation, and rapid acclimation from near-freshwater to highly
538 saline waters involves adjusting the gill gene expression to resemble the osmoregulatory
539 processes typical to the long-term adapted seawater population.
540
541 The second major difference between the two Arabian pupfish populations concerned the
542 immune system, with several genes involved in the inflammatory and immune responses also
543 differentially regulated post-transfer. In teleosts, salinity has been known to have intricate
544 impacts on the immune system. While osmotic stress has been found to increase the nonspecific
545 immune response, a depression of the acquired immune response has also been reported owing
546 to trade-offs in resource allocation (Makrinos & Bowden, 2016). Red Sea population and
547 translocated desert pond fish showed however overexpression of acquired immune response
548 components, such as immunoglobulins (Ig) and major histocompatibility complex class I-
549 related (MR1). The immune response capacities are therefore likely not impacted during
550 acclimation to seawater in Arabian pupfish. Other fishes have been shown to not suffer from
551 immune depression in seawater, such as Nile tilapia *(Oreochromis niloticus*; Dominguez,
552 Takemura, Tsuchiya, & Nakamura, 2004), as well as *Acanthopagrus latus* and *Lates calcarifer*,
553 where plasma Ig levels increase with water salinity (Mozanzadeh et al., 2021). Likewise,
554 hyperosmotic immersion of *Paralichthys olivaceus* boosts branchial major histocompatibility
555 complex expression and the overall mucosal immune response 24 to 48 h post-exposure (Gao,
556 Tang, Sheng, Xing, & Zhan, 2016). Indeed, a crucial role in immunity and defence in teleosts
557 is exerted by mucosal surfaces (Salinas, 2015). Fish gills, skin and gut are coated with a thin
558 mucus layer which acts as a barrier from the surrounding environment and is characterized by

559 physical and antimicrobial defensive functions (Koppang, Kvellestad, & Fischer, 2015;
560 Reverter, Tapissier-Bontemps, Lecchini, Banaigs, & Sasal, 2018), but a role in osmoregulation
561 has also been suggested (Shephard, 1994; Wong et al., 2017). Two mucin-like transcripts were
562 upregulated in Red Sea Arabian pupfish, as well as at 24 h and 7 days post-transfer in desert
563 pond fish. Moreover, several genes related to O-linked glycosylation of mucins,
564 glycosaminoglycan metabolism and mucus production (Malachowicz, Wenne, & Burzynski,
565 2017) were upregulated both in Red Sea individuals and in seawater-exposed desert pond fish.
566 Accordingly, in *Anguilla japonica* mucosal tissues, seawater elicits an increase in mucus cell
567 numbers and secretion, possibly to trap sodium ions (Wong et al., 2017). Similar findings were
568 reported for *Salmo salar*, in addition to salinity-driven modifications of mucin biochemistry
569 (Roberts & Powell, 2003), that were also later described in other euryhaline fishes (Mylonas et
570 al., 2009; Roberts & Powell, 2005). As the molecular results suggest, increased gill mucus
571 production might be at play in seawater in Arabian pupfish and could be another aspect of their
572 acclimation strategy to hyperosmotic environments.
573
574 While osmoregulation and immune response were revealed to be important in long-term
575 adaptation to seawater, a series of short-term and transient response mechanisms were also
576 elicited during the acclimation timeline. Abrupt increases in ion concentration can lead to
577 macromolecular damages in exposed fish epithelia. An increase in sodium, for example, has
578 been linked to cell membrane damages (T. G. Evans & Kultz, 2020) through lipid peroxidation,
579 catalysed by lipoxygenases in response to stress (Kultz, 2005). Two lipoxygenases (ALOXE3,
580 ALOXE15B) were indeed upregulated in Arabian pupfish gills 6 h post-transfer, and were also
581 identified in similar seawater transfer experiments on eels (Kalujnaia et al., 2007). Such
582 membrane disruption can lead to the activation of the so-called cellular stress response (CSR),
583 which encompasses defence mechanisms to protect and repair damaged cellular components

584 and restore homeostasis (T. G. Evans & Kultz, 2020; Kultz, 2005). The CSR machinery
585 responds to sodium-destabilized proteins by overexpressing molecular chaperones, such as
586 heat shock proteins (T. G. Evans & Kultz, 2020), two of which were temporarily upregulated
587 in Arabian pupfish at 24 hours, as well as in a hyperosmotic challenged Sacramento splittail
588 population (Mundy et al., 2020). Rising intracellular sodium levels can also cause nucleic acid
589 structural disruptions (T. G. Evans & Kultz, 2020), and consequently, increased expressions of
590 DNA damage related genes are often reported as part of the CSR following hyperosmotic stress
591 in teleosts (Brennan et al., 2015; Su, Ma, Zhu, Liu, & Gao, 2020; Whitehead et al., 2013). In
592 Arabian pupfish several DNA damage related genes were transiently upregulated especially in
593 the first 24 hours of exposure, like serum/glucocorticoid regulated kinase 1 (SGK1), and
594 similarly increased in other fish following acute seawater challenges (T. G. Evans & Somero,
595 2008; Shaw et al., 2008). Another aspect of hyperosmotic-induced CSR, at least in cultured
596 human cells, is the inhibition of transcriptional and translational activities (Burg et al., 2007).
597 Equivalent to other species, such as the climbing perch (Chen et al., 2018), Arabian pupfish
598 exhibited a downregulation of transcription related genes following seawater exposure, which
599 might be a mechanism to prevent the replication of high salinity-damaged DNA. An inhibition
600 in transcription and translation might also explain the onset of cell cycle arrest that was
601 identified in both Arabian pupfish and climbing perch (Chen et al., 2018) via a downregulation
602 of large sets of cell cycle and mitosis involved genes during the acclimation to seawater. In
603 support of these findings, an immunocytochemistry study in tilapia (*Oreochromis*
604 *mossambicus*) observed a G2 phase arrest in the mitotic cycle of gill cells over a period of 16–
605 72 h post-seawater exposure (Kammerer, Sardella, & Kultz, 2009). Hence, in the first hours of
606 high salinity challenge, gill acclimation in Arabian pupfish is dominated by the onset of
607 macromolecular damages followed by the cellular stress response machinery initiating the
608 repair of the compromised processes to restore homeostasis. Days to weeks after the start of

609 the hyperosmotic challenge, an inhibition of transcriptional activity and simultaneous cell cycle
610 arrest might represent a strategy for the fish to prevent the replication of damaged DNA,
611 preserve energy and buy time to respond to macromolecular damages caused by the increase
612 in ion concentration.
613
614 For longer-term acclimation to seawater, euryhaline fish gills must undergo profound
615 remodelling events in order to switch from an ion absorbing epithelium to an ion secreting one.
616 Arabian pupfish started displaying processes involved in tissue remodelling from the first hours
617 of salinity exposure. Likely to allow a rapid reorganization of the gill epithelium to reverse the
618 ion transport direction, a transient increase in cell proliferation and differentiation related genes
619 was uncovered, as seen in the gills of euryhaline tilapia in the first eight hours of seawater
620 exposure (Kammerer et al., 2009). At the same time, genes involved in keratinization, a process
621 by which keratin accumulate inside epithelial tissue cells to provide barrier-like functions,
622 started to be upregulated. Keratinization gene expression has been found to be salinity
623 dependent in tilapia (Ronkin, Seroussi, Nitzan, Doron-Faigenboim, & Cnaani, 2015) and to be
624 upregulated following air exposure in the amphibious mangrove rivulus skin (*Kryptolebias*
625 *marmoratus*; Dong et al., 2021). Keratinization may represent a strategy to reduce the amount
626 of water loss during dehydration, possibly also following increased environmental salinity, as
627 seen in Arabian pupfish. Programmed cell death, or apoptosis, of high salinity-damaged cells
628 and freshwater-type ionocytes represents another of the first steps in gill epithelium
629 remodelling, essential for full acclimation to seawater (T. G. Evans & Kultz, 2020). A transient
630 upregulation of cytochrome c (CYC) and other genes involved in the mitochondrial apoptotic
631 pathway was seen in Arabian pupfish at 24 hours. This has been previously recorded in
632 mummichog in response to osmotic stresses (Whitehead et al., 2012), and is supported by a
633 microscopy study in Mozambique tilapia revealing increased branchial apoptotic freshwater

ionocytes one day after transfer to seawater (Inokuchi & Kaneko, 2012). At 24 h post-transfer, genes related to cell adhesion began to be upregulated, and cytoskeleton and extracellular matrix organization functions showed increased expression from 72 hours of exposure. Cell adhesion and extracellular matrix pathway upregulation was similarly reported in Sacramento splittails between one and seven days into the acclimation to elevated salinity (Jeffries et al., 2019; Mundy et al., 2020), and branchial cell cytoskeleton reorganization is largely recognized as a fundamental aspect of salinity acclimation in teleosts (T. G. Evans & Somero, 2008; Fiol & Kultz, 2007; Nguyen et al., 2016). As a consequence of tissue remodelling events, an upregulation of mitochondrial respiratory chain and metabolism related genes is also expected to support the increased energy demand, as previously found in similar experiments of euryhaline fish translocation (Chen et al., 2018; Lam et al., 2014; Whitehead et al., 2012). Analogously, in Arabian pupfish there was an overall upregulation of metabolism related genes up to 7 days post-transfer, while genes involved in mitochondrial respiration were overexpressed especially between days one and seven, which is consistent with the time frame for major gill remodelling processes in other species (Foskett et al., 1981; Katoh & Kaneko, 2003; Mundy et al., 2020). In a similar fashion to other euryhaline teleosts, seawater exposed pupfish are therefore affected by transient and longer-lasting gill tissue modifications occurring from the first hours to several days after the beginning of the exposure, and potentially resulting in perdurable modifications which allow longer-term acclimation to the highly saline environment.

Arabian pupfish inhabit profoundly divergent environments of the Arabian Peninsula, ranging from nearly-freshwater ponds found in desert areas to highly saline Red Sea coastal lagoons. The plasticity of these fish under steep increases in water salinity plays a major role in the colonization potential of this species. Remarkably, Arabian pupfish are able to survive flash

659 flood events which likely displace them from desert oases and wash them to the sea, where
660 they eventually establish viable populations (Schunter et al., 2021). By simulating and
661 analysing the exposure to high salinity from near-freshwater over time, not only key processes
662 for a successful acclimation were identified, but also the importance of their timing was
663 uncovered. Arabian pupfish branchial salinity-elicited pathways revealed osmoregulation,
664 immune system and mucus production to be rapid but also long-term acclimation mechanisms
665 to the new environment. In the short-term, cellular stress response processes were triggered,
666 which prevented the fish from suffering permanent damages following acute hyperosmotic
667 exposure. Later in the acclimation, pathways involved in gill epithelium modification and
668 remodelling equipped the organism with lasting adaptations to the increased salinity. While
669 some of the processes occurring during the acclimation timeline resembled mechanisms of
670 seawater exposure previously reported in other euryhaline fish species, others, such as
671 increased mucus production and keratinization, represent less common strategies for high
672 salinity acclimation in teleosts. Overall, the branchial processes revealed in this nearly-
673 freshwater Arabian pupfish population during high salinity acclimation sheds light into this
674 non-model euryhaline species colonization potential of seawater habitats. A large set of
675 differentially timed molecular mechanisms plays a role in the plastic reorganization of the gills
676 in hyperosmotic environments that allows for the expansion of euryhaline teleosts into a wide
677 variety of different habitats.

678
679

References

Benjamini, Y., & Hochberg, Y. (1995). Controlling the false discovery rate - a practical and powerful approach to multiple testing. *Journal of the Royal Statistical Society Series B-Statistical Methodology, 57*(1), 289-300. doi:10.1111/j.2517-6161.1995.tb02031.x

BioBam Bioinformatics. (2019). OmicsBox – Bioinformatics Made Easy. Retrieved from March 3, 2019, https://www.biobam.com/omicsbox

Bœuf, G., & Payan, P. (2001). How should salinity influence fish growth? *Comparative Biochemistry and Physiology Part C: Toxicology & Pharmacology, 130*(4), 411-423. doi:10.1016/s1532-0456(01)00268-x

Bolger, A. M., Lohse, M., & Usadel, B. (2014). Trimmomatic: a flexible trimmer for Illumina sequence data. *Bioinformatics, 30*(15), 2114-2120. doi:10.1093/bioinformatics/btu170

Brennan, R. S., Galvez, F., & Whitehead, A. (2015). Reciprocal osmotic challenges reveal mechanisms of divergence in phenotypic plasticity in the killifish *Fundulus heteroclitus*. *J Exp Biol, 218*(Pt 8), 1212-1222. doi:10.1242/jeb.110445

Burg, M. B., Ferraris, J. D., & Dmitrieva, N. I. (2007). Cellular response to hyperosmotic stresses. *Physiol Rev, 87*(4), 1441-1474. doi:10.1152/physrev.00056.2006

Bystriansky, J. S., Richards, J. G., Schulte, P. M., & Ballantyne, J. S. (2006). Reciprocal expression of gill Na+/K+-ATPase alpha-subunit isoforms alpha1a and alpha1b during seawater acclimation of three salmonid fishes that vary in their salinity tolerance. *J Exp Biol, 209*(Pt 10), 1848-1858. doi:10.1242/jeb.02188

Camacho, C., Coulouris, G., Avagyan, V., Ma, N., Papadopoulos, J., Bealer, K., & Madden, T. L. (2009). BLAST+: architecture and applications. *BMC bioinformatics, 10*(1), 421. doi:10.1186/1471-2105-10-421

Chen, X. L., Lui, E. Y., Ip, Y. K., & Lam, S. H. (2018). RNA sequencing, *de novo* assembly and differential analysis of the gill transcriptome of freshwater climbing perch *Anabas testudineus* after 6 days of seawater exposure. *J Fish Biol, 93*(2), 215-228. doi:10.1111/jfb.13653

Cui, W. X., Ma, A. J., Huang, Z. H., Liu, Z. F., Yang, K., & Zhang, W. (2020). *myo*-inositol facilitates salinity tolerance by modulating multiple physiological functions in the turbot *Scophthalmus maximus*. *Aquaculture, 527*, 735451. doi:10.1016/j.aquaculture.2020.735451

Deane, E. E., & Woo, N. Y. (2004). Differential gene expression associated with euryhalinity in sea bream (*Sparus sarba*). *Am J Physiol Regul Integr Comp Physiol, 287*(5), R1054-1063. doi:10.1152/ajpregu.00347.2004

Delpire, E., & Gagnon, K. B. (2008). SPAK and OSR1: STE20 kinases involved in the regulation of ion homoeostasis and volume control in mammalian cells. *Biochem J, 409*(2), 321-331. doi:10.1042/BJ20071324

Dominguez, M., Takemura, A., Tsuchiya, M., & Nakamura, S. (2004). Impact of different environmental factors on the circulating immunoglobulin levels in the Nile tilapia, *Oreochromis niloticus*. *Aquaculture, 241*(1-4), 491-500. doi:10.1016/j.aquaculture.2004.06.027

Dong, Y. W., Blanchard, T. S., Noll, A., Vasquez, P., Schmitz, J., Kelly, S. P., . . . Whitehead, A. (2021). Genomic and physiological mechanisms underlying skin plasticity during water to air transition in an amphibious fish. *J Exp Biol, 224*(Pt 2), jeb235515. doi:10.1242/jeb.235515

Dymowska, A. K., Hwang, P. P., & Goss, G. G. (2012). Structure and function of ionocytes in the freshwater fish gill. *Respir Physiol Neurobiol, 184*(3), 282-292. doi:10.1016/j.resp.2012.08.025

729 Edwards, S. L., & Marshall, W. S. (2012). Principles and patterns of osmoregulation and
730 euryhalinity in fishes. In A. P. F. Stephen D. McCormick & J. B. Colin (Eds.),
731 *Euryhaline Fishes* (Vol. 32, pp. 1-44): Academic Press.
732 Evans, D. H., Piermarini, P. M., & Choe, K. P. (2005). The multifunctional fish gill:
733 dominant site of gas exchange, osmoregulation, acid-base regulation, and excretion of
734 nitrogenous waste. *Physiol Rev, 85*(1), 97-177. doi:10.1152/physrev.00050.2003
735 Evans, T. G., & Kultz, D. (2020). The cellular stress response in fish exposed to salinity
736 fluctuations. *J Exp Zool A Ecol Integr Physiol, 333*(6), 421-435. doi:10.1002/jez.2350
737 Evans, T. G., & Somero, G. N. (2008). A microarray-based transcriptomic time-course of
738 hyper- and hypo-osmotic stress signaling events in the euryhaline fish *Gillichthys*
739 *mirabilis*: osmosensors to effectors. *J Exp Biol, 211*(Pt 22), 3636-3649.
740 doi:10.1242/jeb.022160
741 Finn, R. D., Clements, J., & Eddy, S. R. (2011). HMMER web server: interactive sequence
742 similarity searching. *Nucleic Acids Res, 39*(Web Server issue), W29-37.
743 doi:10.1093/nar/gkr367
744 Fiol, D. F., & Kultz, D. (2007). Osmotic stress sensing and signaling in fishes. *FEBS J,*
745 *274*(22), 5790-5798. doi:10.1111/j.1742-4658.2007.06099.x
746 Fischer, D. S., Theis, F. J., & Yosef, N. (2018). Impulse model-based differential expression
747 analysis of time course sequencing data. *Nucleic Acids Res, 46*(20), e119.
748 doi:10.1093/nar/gky675
749 Flemmer, A. W., Monette, M. Y., Djurisic, M., Dowd, B., Darman, R., Gimenez, I., &
750 Forbush, B. (2010). Phosphorylation state of the Na+-K+-Cl- cotransporter (NKCC1)
751 in the gills of Atlantic killifish (*Fundulus heteroclitus*) during acclimation to water of
752 varying salinity. *J Exp Biol, 213*(Pt 9), 1558-1566. doi:10.1242/jeb.039644
753 Foskett, J. K., Logsdon, C. D., Turner, T., Machen, T. E., & Bern, H. A. (1981).
754 Differentiation of the chloride extrusion mechanism during seawater adaptation of a
755 teleost fish, the cichlid *Sarotherodon mossambicus*. *Journal of Experimental Biology,*
756 *93*(1), 209-224.
757 Fu, L., Niu, B., Zhu, Z., Wu, S., & Li, W. (2012). CD-HIT: accelerated for clustering the
758 next-generation sequencing data. *Bioinformatics, 28*(23), 3150-3152.
759 doi:10.1093/bioinformatics/bts565
760 Gao, Y., Tang, X., Sheng, X., Xing, J., & Zhan, W. (2016). Antigen uptake and expression of
761 antigen presentation-related immune genes in flounder (*Paralichthys olivaceus*) after
762 vaccination with an inactivated *Edwardsiella tarda* immersion vaccine, following
763 hyperosmotic treatment. *Fish Shellfish Immunol, 55*, 274-280.
764 doi:10.1016/j.fsi.2016.05.042
765 Gotz, S., Garcia-Gomez, J. M., Terol, J., Williams, T. D., Nagaraj, S. H., Nueda, M. J., . . .
766 Conesa, A. (2008). High-throughput functional annotation and data mining with the
767 Blast2GO suite. *Nucleic Acids Res, 36*(10), 3420-3435. doi:10.1093/nar/gkn176
768 Grabherr, M. G., Haas, B. J., Yassour, M., Levin, J. Z., Thompson, D. A., Amit, I., . . . Zeng,
769 Q. (2011). Trinity: reconstructing a full-length transcriptome without a genome from
770 RNA-Seq data. *Nature biotechnology, 29*(7), 644.
771 Haas, B. J., Papanicolaou, A., Yassour, M., Grabherr, M., Blood, P. D., Bowden, J., . . .
772 Regev, A. (2013). *De novo* transcript sequence reconstruction from RNA-seq using
773 the Trinity platform for reference generation and analysis. *Nat Protoc, 8*(8), 1494-
774 1512. doi:10.1038/nprot.2013.084
775 Hiroi, J., & McCormick, S. D. (2012). New insights into gill ionocyte and ion transporter
776 function in euryhaline and diadromous fish. *Respir Physiol Neurobiol, 184*(3), 257-
777 268. doi:10.1016/j.resp.2012.07.019

778 Hrbek, T., & Meyer, A. (2003). Closing of the Tethys Sea and the phylogeny of Eurasian
779 killifishes (Cyprinodontiformes: Cyprinodontidae). *J Evol Biol, 16*(1), 17-36.
780 doi:10.1046/j.1420-9101.2003.00475.x
781 Hsu, H. H., Lin, L. Y., Tseng, Y. C., Horng, J. L., & Hwang, P. P. (2014). A new model for
782 fish ion regulation: identification of ionocytes in freshwater- and seawater-acclimated
783 medaka (*Oryzias latipes*). *Cell Tissue Res, 357*(1), 225-243. doi:10.1007/s00441-014-
784 1883-z
785 Huerta-Cepas, J., Szklarczyk, D., Heller, D., Hernandez-Plaza, A., Forslund, S. K., Cook, H.,
786 . . . Bork, P. (2019). eggNOG 5.0: a hierarchical, functionally and phylogenetically
787 annotated orthology resource based on 5090 organisms and 2502 viruses. *Nucleic*
788 *Acids Res, 47*(D1), D309-D314. doi:10.1093/nar/gky1085
789 Hwang, P. P., Lee, T. H., & Lin, L. Y. (2011). Ion regulation in fish gills: recent progress in
790 the cellular and molecular mechanisms. *Am J Physiol Regul Integr Comp Physiol,*
791 *301*(1), R28-47. doi:10.1152/ajpregu.00047.2011
792 Hwang, P. P., & Lin, L. Y. (2013). Gill ionic transport, acid-base regulation, and nitrogen
793 excretion. In D. H. Evans, J. B. Claiborne, & S. Currie (Eds.), *The physiology of*
794 *fishes* (Vol. 4, pp. 205-233): CRC Press.
795 Inokuchi, M., & Kaneko, T. (2012). Recruitment and degeneration of mitochondrion-rich
796 cells in the gills of Mozambique tilapia *Oreochromis mossambicus* during adaptation
797 to a hyperosmotic environment. *Comp Biochem Physiol A Mol Integr Physiol, 162*(3),
798 245-251. doi:10.1016/j.cbpa.2012.03.018
799 Ip, Y. K., Loong, A. M., Kuah, J. S., Sim, E. W., Chen, X. L., Wong, W. P., . . . Chew, S. F.
800 (2012). Roles of three branchial Na(+)-K(+)-ATPase alpha-subunit isoforms in
801 freshwater adaptation, seawater acclimation, and active ammonia excretion in *Anabas*
802 *testudineus*. *Am J Physiol Regul Integr Comp Physiol, 303*(1), R112-125.
803 doi:10.1152/ajpregu.00618.2011
804 Jeffries, K. M., Connon, R. E., Verhille, C. E., Dabruzzi, T. F., Britton, M. T., Durbin-
805 Johnson, B. P., & Fangue, N. A. (2019). Divergent transcriptomic signatures in
806 response to salinity exposure in two populations of an estuarine fish. *Evol Appl, 12*(6),
807 1212-1226. doi:10.1111/eva.12799
808 Kalujnaia, S., McVee, J., Kasciukovic, T., Stewart, A. J., & Cramb, G. (2010). A role for
809 inositol monophosphatase 1 (IMPA1) in salinity adaptation in the euryhaline eel
810 (*Anguilla anguilla*). *FASEB J, 24*(10), 3981-3991. doi:10.1096/fj.10-161000
811 Kalujnaia, S., McWilliam, I. S., Zaguinaiko, V. A., Feilen, A. L., Nicholson, J., Hazon, N., . .
812 . Cramb, G. (2007). Transcriptomic approach to the study of osmoregulation in the
813 European eel *Anguilla anguilla*. *Physiol Genomics, 31*(3), 385-401.
814 doi:10.1152/physiolgenomics.00059.2007
815 Kammerer, B. D., Sardella, B. A., & Kultz, D. (2009). Salinity stress results in rapid cell
816 cycle changes of tilapia (*Oreochromis mossambicus*) gill epithelial cells. *J Exp Zool A*
817 *Ecol Genet Physiol, 311*(2), 80-90. doi:10.1002/jez.498
818 Katoh, F., & Kaneko, T. (2003). Short-term transformation and long-term replacement of
819 branchial chloride cells in killifish transferred from seawater to freshwater, revealed
820 by morphofunctional observations and a newly established 'time-differential double
821 fluorescent staining' technique. *J Exp Biol, 206*(Pt 22), 4113-4123.
822 doi:10.1242/jeb.00659
823 Komoroske, L. M., Jeffries, K. M., Connon, R. E., Dexter, J., Hasenbein, M., Verhille, C., &
824 Fangue, N. A. (2016). Sublethal salinity stress contributes to habitat limitation in an
825 endangered estuarine fish. *Evol Appl, 9*(8), 963-981. doi:10.1111/eva.12385

826 Koppang, E. O., Kvellestad, A., & Fischer, U. (2015). Fish mucosal immunity: gill. In B. H.
827 Beck & E. Peatman (Eds.), *Mucosal Health in Aquaculture* (pp. 93-133). San Diego:
828 Academic Press.
829 Kozak, G. M., Brennan, R. S., Berdan, E. L., Fuller, R. C., & Whitehead, A. (2014).
830 Functional and population genomic divergence within and between two species of
831 killifish adapted to different osmotic niches. *Evolution, 68*(1), 63-80.
832 doi:10.1111/evo.12265
833 Kultz, D. (2005). Molecular and evolutionary basis of the cellular stress response. *Annu Rev*
834 *Physiol, 67*(1), 225-257. doi:10.1146/annurev.physiol.67.040403.103635
835 Kultz, D. (2012). The combinatorial nature of osmosensing in fishes. *Physiology (Bethesda),*
836 *27*(4), 259-275. doi:10.1152/physiol.00014.2012
837 Kultz, D. (2015). Physiological mechanisms used by fish to cope with salinity stress. *J Exp*
838 *Biol, 218*(Pt 12), 1907-1914. doi:10.1242/jeb.118695
839 Lafond-Lapalme, J., Duceppe, M. O., Wang, S., Moffett, P., & Mimee, B. (2017). A new
840 method for decontamination of *de novo* transcriptomes using a hierarchical clustering
841 algorithm. *Bioinformatics, 33*(9), 1293-1300. doi:10.1093/bioinformatics/btw793
842 Lam, S. H., Lui, E. Y., Li, Z., Cai, S., Sung, W. K., Mathavan, S., . . . Ip, Y. K. (2014).
843 Differential transcriptomic analyses revealed genes and signaling pathways involved
844 in iono-osmoregulation and cellular remodeling in the gills of euryhaline
845 Mozambique tilapia, *Oreochromis mossambicus*. *BMC Genomics, 15*(1), 921.
846 doi:10.1186/1471-2164-15-921
847 Langmead, B., & Salzberg, S. L. (2012). Fast gapped-read alignment with Bowtie 2. *Nat*
848 *Methods, 9*(4), 357-359. doi:10.1038/nmeth.1923
849 Leguen, I., Le Cam, A., Montfort, J., Peron, S., & Fautrel, A. (2015). Transcriptomic analysis
850 of trout gill ionocytes in fresh water and sea water using laser capture microdissection
851 combined with microarray analysis. *PLoS One, 10*(10), e0139938.
852 doi:10.1371/journal.pone.0139938
853 Lema, S. C., Carvalho, P. G., Egelston, J. N., Kelly, J. T., & McCormick, S. D. (2018).
854 Dynamics of gene expression responses for ion transport proteins and aquaporins in
855 the gill of a euryhaline pupfish during freshwater and high-salinity acclimation.
856 *Physiol Biochem Zool, 91*(6), 1148-1171. doi:10.1086/700432
857 Li, J., Xue, L., Cao, M., Zhang, Y., Wang, Y., Xu, S., . . . Lou, Z. (2020). Gill transcriptomes
858 reveal expression changes of genes related with immune and ion transport under
859 salinity stress in silvery pomfret (*Pampus argenteus*). *Fish Physiol Biochem, 46*(4),
860 1255-1277. doi:10.1007/s10695-020-00786-9
861 Lotan, R. (1969). Sodium, chloride and water balance in the euryhaline teleost *Aphanius*
862 *dispar* (Rüppell) (Cyprinodontidae). *Zeitschrift für vergleichende Physiologie, 65*(4),
863 455-462. doi:10.1007/bf00299054
864 Lotan, R. (1971). Osmotic adjustment in the euryhaline teleost *Aphanius dispar*
865 (Cyprinodontidae). *Zeitschrift für vergleichende Physiologie, 75*(4), 383-387.
866 doi:10.1007/bf00630558
867 Love, M. I., Huber, W., & Anders, S. (2014). Moderated estimation of fold change and
868 dispersion for RNA-seq data with DESeq2. *Genome Biol, 15*(12), 550.
869 doi:10.1186/s13059-014-0550-8
870 Ma, A., Cui, W., Wang, X., Zhang, W., Liu, Z., Zhang, J., & Zhao, T. (2020).
871 Osmoregulation by the *myo*-inositol biosynthesis pathway in turbot *Scophthalmus*
872 *maximus* and its regulation by anabolite and c-Myc. *Comp Biochem Physiol A Mol*
873 *Integr Physiol, 242*, 110636. doi:10.1016/j.cbpa.2019.110636
874 Makrinos, D. L., & Bowden, T. J. (2016). Natural environmental impacts on teleost immune
875 function. *Fish Shellfish Immunol, 53*, 50-57. doi:10.1016/j.fsi.2016.03.008

876 Malachowicz, M., Wenne, R., & Burzynski, A. (2017). *De novo* assembly of the sea trout
877 (*Salmo trutta m. trutta*) skin transcriptome to identify putative genes involved in the
878 immune response and epidermal mucus secretion. *PLoS One, 12*(2), e0172282.
879 doi:10.1371/journal.pone.0172282
880 Marshall, W. S. (2011). Mechanosensitive signalling in fish gill and other ion transporting
881 epithelia. *Acta Physiol (Oxf), 202*(3), 487-499. doi:10.1111/j.1748-1716.2010.02189.x
882 McCormick, S. D., Regish, A. M., & Christensen, A. K. (2009). Distinct freshwater and
883 seawater isoforms of Na+/K+-ATPase in gill chloride cells of Atlantic salmon. *J Exp*
884 *Biol, 212*(Pt 24), 3994-4001. doi:10.1242/jeb.037275
885 Morgan, J. D., & Iwama, G. K. (1991). Effects of salinity on growth, metabolism, and ion
886 regulation in juvenile rainbow and steelhead trout (*Oncorhynchus mykiss*) and fall
887 chinook salmon (*Oncorhynchus tshawytscha*). *Canadian Journal of Fisheries and*
888 *Aquatic Sciences, 48*(11), 2083-2094. doi:doi:10.1139/f91-247
889 Mozanzadeh, M. T., Safari, O., Oosooli, R., Mehrjooyan, S., Najafabadi, M. Z., Hoseini, S.
890 J., . . . Monem, J. (2021). The effect of salinity on growth performance, digestive and
891 antioxidant enzymes, humoral immunity and stress indices in two euryhaline fish
892 species: Yellowfin seabream (*Acanthopagrus latus*) and Asian seabass (*Lates*
893 *calcarifer*). *Aquaculture, 534*, 736329. doi:10.1016/j.aquaculture.2020.736329
894 Mundy, P. C., Jeffries, K. M., Fangue, N. A., & Connon, R. E. (2020). Differential regulation
895 of select osmoregulatory genes and Na(+)/K(+)-ATPase paralogs may contribute to
896 population differences in salinity tolerance in a semi-anadromous fish. *Comp Biochem*
897 *Physiol A Mol Integr Physiol, 240*, 110584. doi:10.1016/j.cbpa.2019.110584
898 Mylonas, C. C., Pavlidis, M., Papandroulakis, N., Zaiss, M. M., Tsafarakis, D., Papadakis, I.
899 E., & Varsamos, S. (2009). Growth performance and osmoregulation in the shi drum
900 (*Umbrina cirrosa*) adapted to different environmental salinities. *Aquaculture, 287*(1-
901 2), 203-210. doi:10.1016/j.aquaculture.2008.10.024
902 Nguyen, T. V., Jung, H., Nguyen, T. M., Hurwood, D., & Mather, P. (2016). Evaluation of
903 potential candidate genes involved in salinity tolerance in striped catfish
904 (*Pangasianodon hypophthalmus*) using an RNA-Seq approach. *Mar Genomics, 25*,
905 75-88. doi:10.1016/j.margen.2015.11.010
906 Patro, R., Duggal, G., Love, M. I., Irizarry, R. A., & Kingsford, C. (2017). Salmon provides
907 fast and bias-aware quantification of transcript expression. *Nat Methods, 14*(4), 417-
908 419. doi:10.1038/nmeth.4197
909 Plaut, I. (2000). Resting metabolic rate, critical swimming speed, and routine activity of the
910 euryhaline cyprinodontid, *Aphanius dispar*, acclimated to a wide range of salinities.
911 *Physiol Biochem Zool, 73*(5), 590-596. doi:10.1086/317746
912 Reverter, M., Tapissier-Bontemps, N., Lecchini, D., Banaigs, B., & Sasal, P. (2018).
913 Biological and ecological roles of external fish mucus: a review. *Fishes, 3*(4), 41.
914 doi:10.3390/fishes3040041
915 Richards, J. G., Semple, J. W., Bystriansky, J. S., & Schulte, P. M. (2003). Na+/K+-ATPase
916 alpha-isoform switching in gills of rainbow trout (*Oncorhynchus mykiss*) during
917 salinity transfer. *J Exp Biol, 206*(Pt 24), 4475-4486. doi:10.1242/jeb.00701
918 Rinehart, J., Vazquez, N., Kahle, K. T., Hodson, C. A., Ring, A. M., Gulcicek, E. E., . . .
919 Lifton, R. P. (2011). WNK2 kinase is a novel regulator of essential neuronal cation-
920 chloride cotransporters. *J Biol Chem, 286*(34), 30171-30180.
921 doi:10.1074/jbc.M111.222893
922 Roberts, S. D., & Powell, M. D. (2003). Comparative ionic flux and gill mucous cell
923 histochemistry: effects of salinity and disease status in Atlantic salmon (*Salmo salar*
924 L.). *Comp Biochem Physiol A Mol Integr Physiol, 134*(3), 525-537.
925 doi:10.1016/s1095-6433(02)00327-6

926 Roberts, S. D., & Powell, M. D. (2005). The viscosity and glycoprotein biochemistry of
927 salmonid mucus varies with species, salinity and the presence of amoebic gill disease.
928 *J Comp Physiol B, 175*(1), 1-11. doi:10.1007/s00360-004-0453-1
929 Ronkin, D., Seroussi, E., Nitzan, T., Doron-Faigenboim, A., & Cnaani, A. (2015). Intestinal
930 transcriptome analysis revealed differential salinity adaptation between two tilapiine
931 species. *Comp Biochem Physiol Part D Genomics Proteomics, 13*, 35-43.
932 doi:10.1016/j.cbd.2015.01.003
933 Salinas, I. (2015). The mucosal immune system of teleost fish. *Biology, 4*(3), 525-539.
934 doi:10.3390/biology4030525
935 Schultz, E. T., & McCormick, S. D. (2012). Euryhalinity in an evolutionary context. In A. P.
936 F. Stephen D. McCormick & J. B. Colin (Eds.), *Euryhaline Fishes* (Vol. 32, pp. 477-
937 533): Academic Press.
938 Schunter, C., Bonzi, L. C., Norstog, J., Sourisse, J., Berumen, M. L., Angel, Y., . . . Ravasi,
939 T. (2021). Desert fish populations tolerate extreme salinity change to overcome
940 hydrological constraints. *bioRxiv*, 2021.2005.2014.444120.
941 doi:10.1101/2021.05.14.444120
942 Scott, G. R., Claiborne, J. B., Edwards, S. L., Schulte, P. M., & Wood, C. M. (2005). Gene
943 expression after freshwater transfer in gills and opercular epithelia of killifish: insight
944 into divergent mechanisms of ion transport. *J Exp Biol, 208*(Pt 14), 2719-2729.
945 doi:10.1242/jeb.01688
946 Scott, G. R., Richards, J. G., Forbush, B., Isenring, P., & Schulte, P. M. (2004). Changes in
947 gene expression in gills of the euryhaline killifish *Fundulus heteroclitus* after abrupt
948 salinity transfer. *Am J Physiol Cell Physiol, 287*(2), C300-309.
949 doi:10.1152/ajpcell.00054.2004
950 Shaw, J. R., Sato, J. D., VanderHeide, J., LaCasse, T., Stanton, C. R., Lankowski, A., . . .
951 Stanton, B. A. (2008). The role of SGK and CFTR in acute adaptation to seawater in
952 *Fundulus heteroclitus*. *Cell Physiol Biochem, 22*(1-4), 69-78. doi:10.1159/000149784
953 Shephard, K. L. (1994). Functions for fish mucus. *Reviews in Fish Biology and Fisheries,*
954 *4*(4), 401-429. doi:10.1007/Bf00042888
955 Simao, F. A., Waterhouse, R. M., Ioannidis, P., Kriventseva, E. V., & Zdobnov, E. M.
956 (2015). BUSCO: assessing genome assembly and annotation completeness with
957 single-copy orthologs. *Bioinformatics, 31*(19), 3210-3212.
958 doi:10.1093/bioinformatics/btv351
959 Soneson, C., Love, M. I., & Robinson, M. D. (2015). Differential analyses for RNA-seq:
960 transcript-level estimates improve gene-level inferences. *F1000Research, 4*.
961 doi:10.12688/f1000research.7563.1
962 Song, L., & Florea, L. (2015). Rcorrector: efficient and accurate error correction for Illumina
963 RNA-seq reads. *GigaScience, 4*(1), 48. doi:10.1186/s13742-015-0089-y
964 Su, H., Ma, D., Zhu, H., Liu, Z., & Gao, F. (2020). Transcriptomic response to three osmotic
965 stresses in gills of hybrid tilapia (*Oreochromis mossambicus* female x *O. urolepis*
966 *hornorum* male). *BMC Genomics, 21*(1), 110. doi:10.1186/s12864-020-6512-5
967 Takei, Y., & Hwang, P.-P. (2016). Homeostatic responses to osmotic stress. In C. B. Schreck,
968 L. Tort, A. P. Farrell, & C. J. Brauner (Eds.), *Biology of Stress in Fish - Fish*
969 *Physiology* (Vol. 35, pp. 207-249): Academic Press.
970 Tine, M., Bonhomme, F., McKenzie, D. J., & Durand, J. D. (2010). Differential expression of
971 the heat shock protein Hsp70 in natural populations of the tilapia, *Sarotherodon*
972 *melanotheron*, acclimatised to a range of environmental salinities. *BMC Ecol, 10*(1),
973 11. doi:10.1186/1472-6785-10-11

Tipsmark, C. K., Breves, J. P., Seale, A. P., Lerner, D. T., Hirano, T., & Grau, E. G. (2011). Switching of Na+, K+-ATPase isoforms by salinity and prolactin in the gill of a cichlid fish. *J Endocrinol, 209*(2), 237-244. doi:10.1530/JOE-10-0495

Tseng, Y. C., & Hwang, P. P. (2008). Some insights into energy metabolism for osmoregulation in fish. *Comp Biochem Physiol C Toxicol Pharmacol, 148*(4), 419-429. doi:10.1016/j.cbpc.2008.04.009

Uchida, K., Kaneko, T., Miyazaki, H., Hasegawa, S., & Hirano, T. (2000). Excellent salinity tolerance of mozambique tilapia (*Oreochromis mossambicus*): elevated chloride cell activity in the branchial and opercular epithelia of the fish adapted to concentrated seawater. *Zoological Science, 17*(2), 149-160. doi:10.2108/zsj.17.149

Urbina, M. A., Schulte, P. M., Bystriansky, J. S., & Glover, C. N. (2013). Differential expression of Na+, K(+)-ATPase alpha-1 isoforms during seawater acclimation in the amphidromous galaxiid fish *Galaxias maculatus*. *J Comp Physiol B, 183*(3), 345-357. doi:10.1007/s00360-012-0719-y

Velotta, J. P., Wegrzyn, J. L., Ginzburg, S., Kang, L., Czesny, S., O'Neill, R. J., . . . Schultz, E. T. (2017). Transcriptomic imprints of adaptation to fresh water: parallel evolution of osmoregulatory gene expression in the Alewife. *Mol Ecol, 26*(3), 831-848. doi:10.1111/mec.13983

Wang, Y. F., Yan, J. J., Tseng, Y. C., Chen, R. D., & Hwang, P. P. (2015). Molecular physiology of an extra-renal Cl(-) uptake mechanism for body fluid Cl(-) homeostasis. *Int J Biol Sci, 11*(10), 1190-1203. doi:10.7150/ijbs.11737

Whitehead, A., Roach, J. L., Zhang, S., & Galvez, F. (2011). Genomic mechanisms of evolved physiological plasticity in killifish distributed along an environmental salinity gradient. *Proc Natl Acad Sci U S A, 108*(15), 6193-6198. doi:10.1073/pnas.1017542108

Whitehead, A., Roach, J. L., Zhang, S., & Galvez, F. (2012). Salinity- and population-dependent genome regulatory response during osmotic acclimation in the killifish (*Fundulus heteroclitus*) gill. *J Exp Biol, 215*(Pt 8), 1293-1305. doi:10.1242/jeb.062075

Whitehead, A., Zhang, S., Roach, J. L., & Galvez, F. (2013). Common functional targets of adaptive micro- and macro-evolutionary divergence in killifish. *Mol Ecol, 22*(14), 3780-3796. doi:10.1111/mec.12316

Wong, M. K. S., Tsukada, T., Ogawa, N., Pipil, S., Ozaki, H., Suzuki, Y., . . . Takei, Y. (2017). A sodium binding system alleviates acute salt stress during seawater acclimation in eels. *Zoological Lett, 3*(1), 22. doi:10.1186/s40851-017-0081-8

Yancey, P. H., Clark, M. E., Hand, S. C., Bowlus, R. D., & Somero, G. N. (1982). Living with water stress: evolution of osmolyte systems. *Science, 217*(4566), 1214-1222. doi:10.1126/science.7112124

Zhu, A., Ibrahim, J. G., & Love, M. I. (2019). Heavy-tailed prior distributions for sequence count data: removing the noise and preserving large differences. *Bioinformatics, 35*(12), 2084-2092. doi:10.1093/bioinformatics/bty895

Acknowledgements

This study was supported by the King Abdullah University of Science and Technology (KAUST). The project was completed under KAUST ethics permit 15IBEC35_Ravasi. We thank KAUST Coastal and Marine Resources Core Lab and Jessica L. Norstog for assistance with animal collection and maintenance. We also thank KAUST Bioscience Core Lab for assistance with Illumina library preparation and sequencing. The authors declare there are no conflicts of interest.

Author contributions

L.C.B., A.A.M., C.S. conceived, designed and performed the experiment, with input from T.R. L.C.B. and C.S. performed the sample collection. L.C.B. and A.A.M. prepared the samples for RNA sequencing. L.C.B. analyzed the data, with input from C.S. and R.L. L.C.B. interpreted the data and wrote the manuscript, with input from C.S. All authors provided input to and approved the final version of the manuscript.

Data archiving statement

Raw sequence data are available through the National Center for Biotechnology Information Sequence Read Archive under BioProject PRJNA722804.

Competing interests

The authors declare no competing interests.

1039 Figure legends

1040

1041 Figure 1. Sampling locations and target organism. (a) Map of the region with inset (b) showing
1042 the specific sampling locations in the central western region of Saudi Arabia. (c) Photos of the
1043 sampling sites. (d) Pictures of collected male (top) and female (bottom) Arabian pupfish.

1044

1045 Figure 2. Experimental design. a) Fish from desert pond (DP) kept in native water salinity (1.9
1046 ppt) were sampled at time 0 b) Fish from Red Sea lagoon (RS) kept in native water salinity (43
1047 ppt) were sampled at time 0 c) Fish from desert pond transferred to seawater (43 ppt) were
1048 sampled at 5 different time points. A total of 33 samples were analyzed.

1049

1050 Figure 3. Principal component analysis (PCA) of variance stabilized expression values for the
1051 gills of desert pond (n=4) and Red Sea coastal lagoon (n=6) *Aphanius dispar* individuals at
1052 time 0. 44% of the total variation is explained by the first two components.

1053

1054 Figure 4. Numbers of differentially expressed genes in pairwise comparisons of desert pond
1055 fish controls (0 h) versus seawater exposed fish at different time points (6 h, 24 h, 72 h, 7 d, 21
1056 d) and Red Sea (RS) population, and consecutive post-transfer time points.

1057

1058 Figure 5. Heatmap of transiently (A) or monotonously (B) up-(↑) and down- (↓) regulated
1059 differentially expressed genes over the experimental timeline, as identified by ImpulseDE2
1060 analysis. DP and RS stand for desert pond and Red Sea samples, respectively.

1061

1062 Figure 6. Changes in ratio and expression direction of differentially expressed genes grouped
1063 by functions along the acclimation timeline. The circle sizes are proportional to the gene
1064 number ratio for a specific function at a certain time point; the circle colours correspond to the
1065 ratio of the upregulated (red) vs downregulated (blue) genes for the function at that time point.

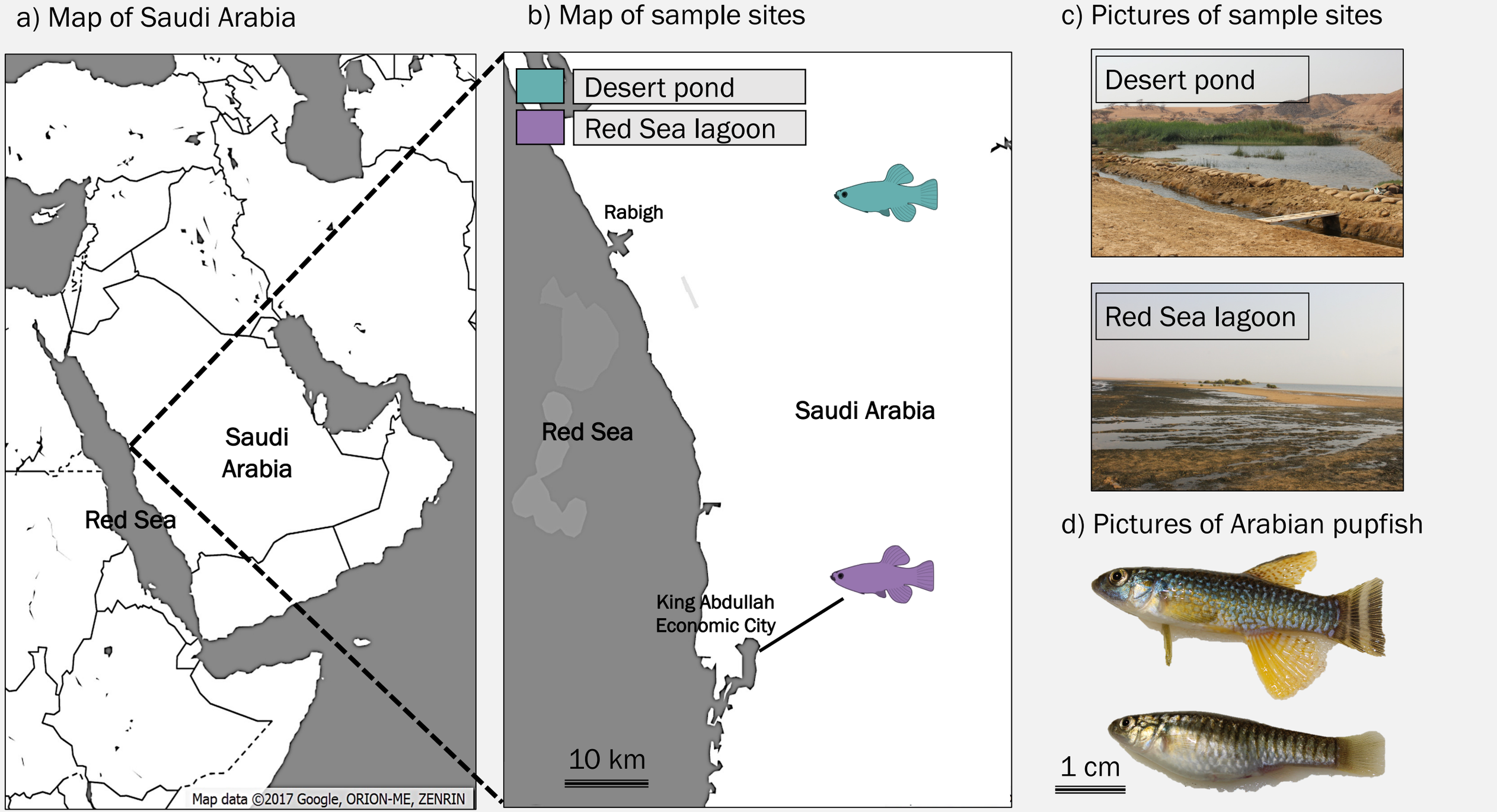
a) Map of Saudi Arabia
b) Map of sample sites
c) Pictures of sample sites
Saudi Arabia
Red Sea
Map data ©2017 Google, ORION-ME, ZENRIN
Desert pond
Red Sea lagoon
Rabigh
Red Sea
Saudi Arabia
King Abdullah Economic City
10 km
Desert pond
Red Sea lagoon
d) Pictures of Arabian pupfish
1 cm

a) Desert pond controls

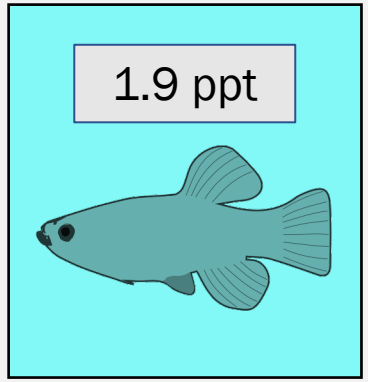

0 h
DP

b) Red Sea controls

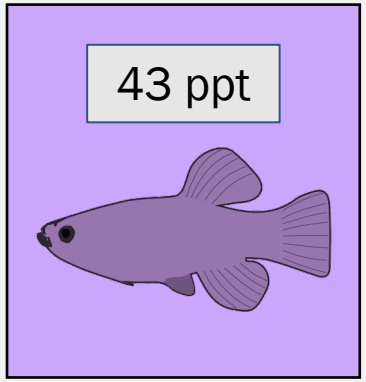

0 h
RS

c) Desert pond fish transferred to seawater

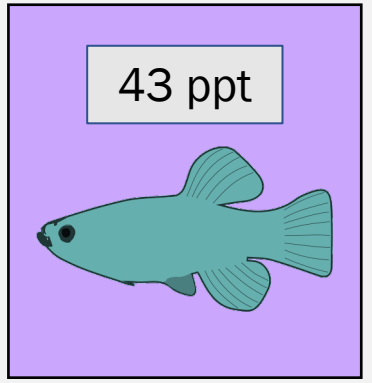

6 h	24 h	72 h	7 d	21 d

N = 33

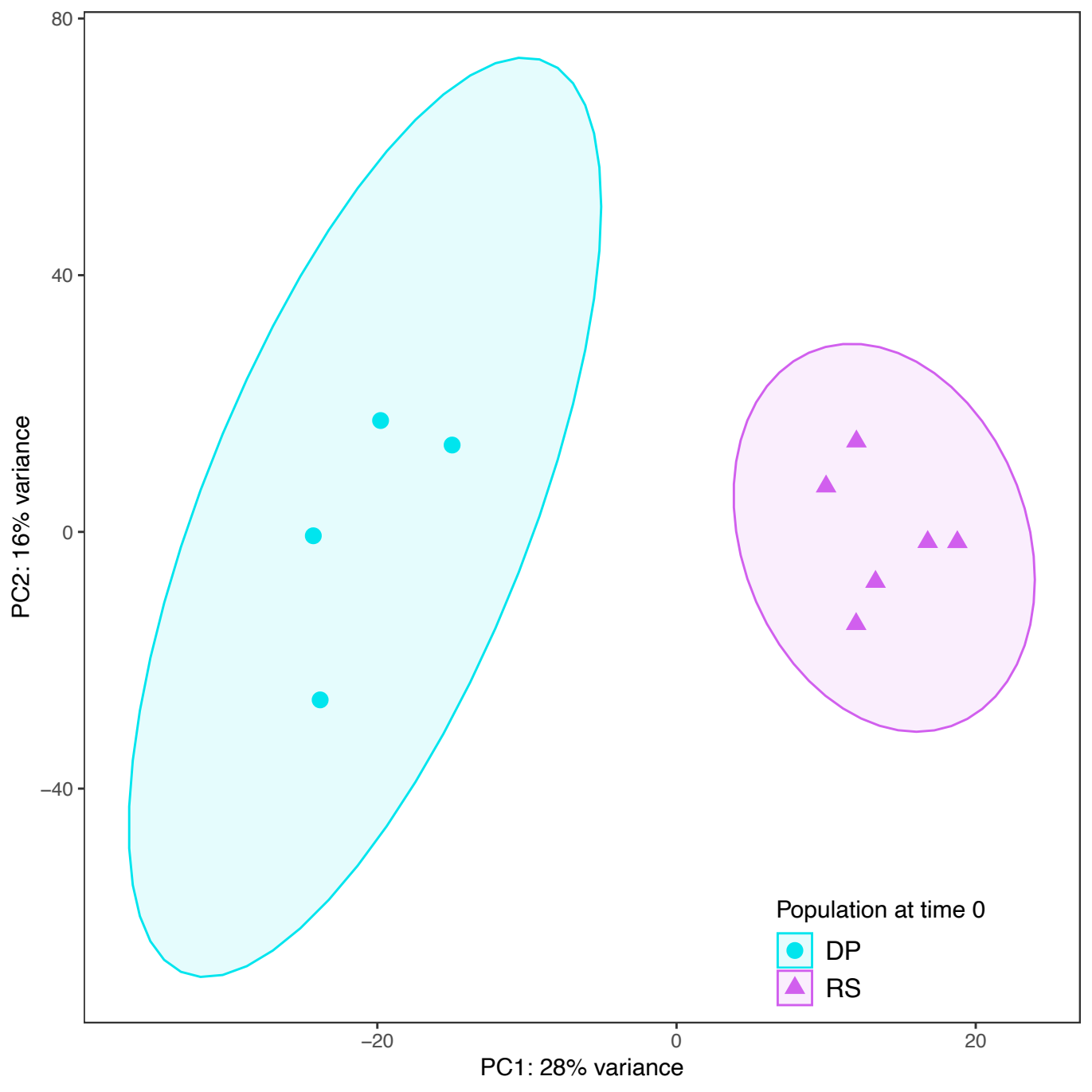
80
40
0
−40
PC2: 16% variance
−20
0
20
PC1: 28% variance
Population at time 0
DP
RS

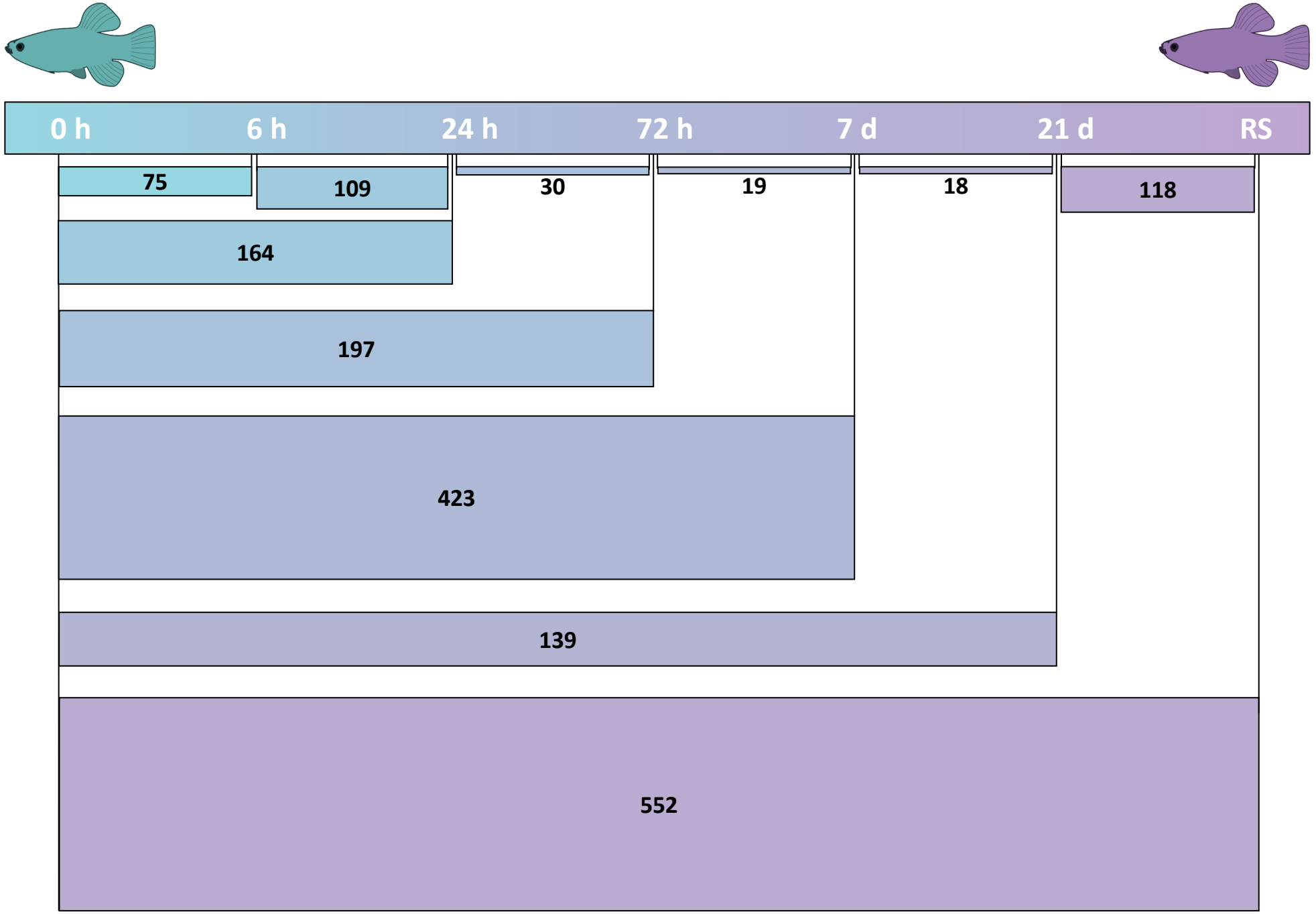
0 h
6 h
24 h
72 h
7 d
21 d
RS
75
109
30
19
18
118
164
197
423
139
552

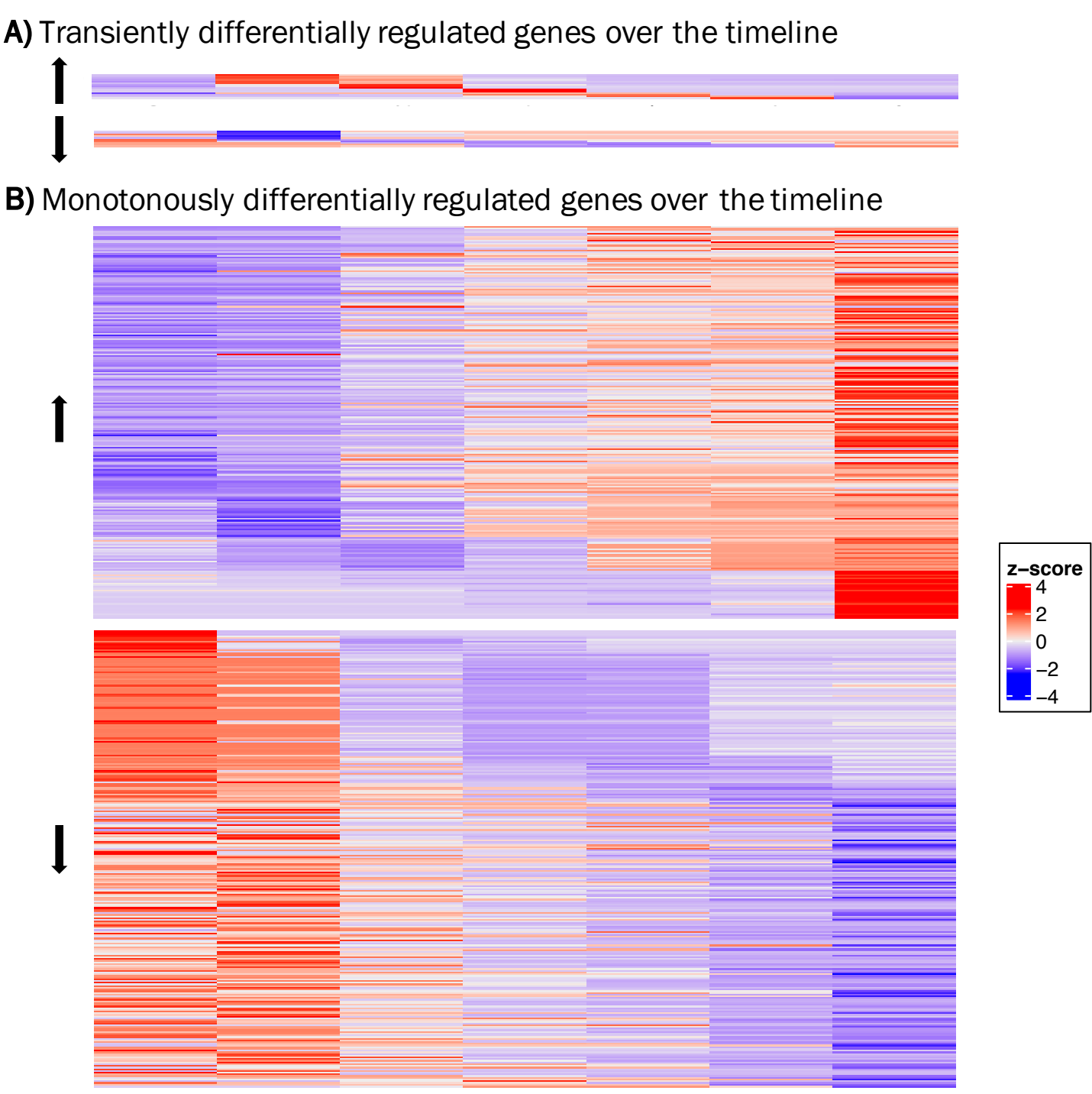
A) Transiently differentially regulated genes over the timeline
B) Monotonously differentially regulated genes over the timeline
z–score
4
2
0
−2
−4

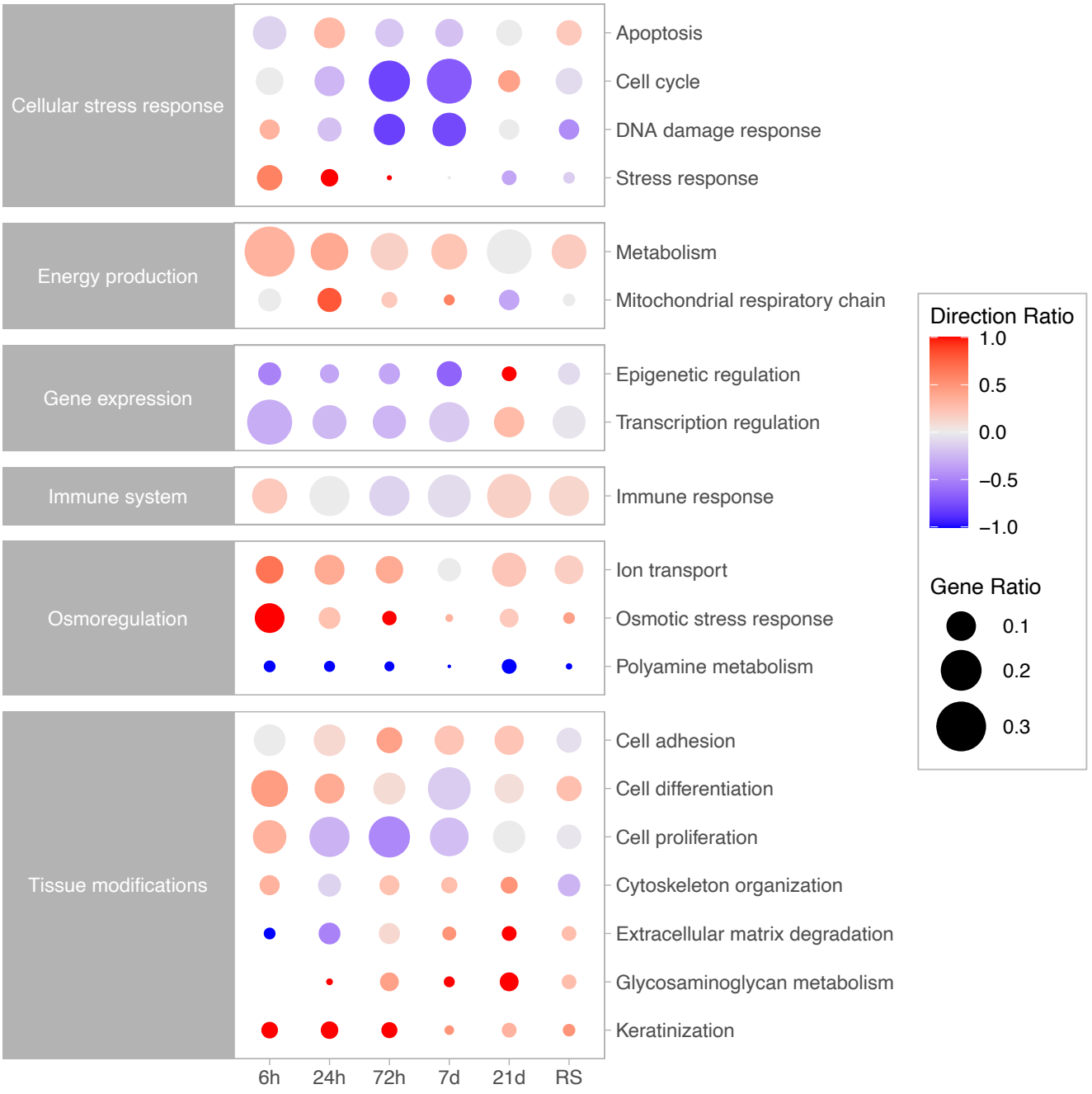
Cellular stress response
Apoptosis
Cell cycle
DNA damage response
Stress response
Energy production
Metabolism
Mitochondrial respiratory chain
Gene expression
Epigenetic regulation
Transcription regulation
Immune system
Immune response
Osmoregulation
Ion transport
Osmotic stress response
Polyamine metabolism
Tissue modifications
Cell adhesion
Cell differentiation
Cell proliferation
Cytoskeleton organization
Extracellular matrix degradation
Glycosaminoglycan metabolism
Keratinization
6h
24h
72h
7d
21d
RS
Direction Ratio
1.0
0.5
0.0
−0.5
−1.0
Gene Ratio
0.1
0.2
0.3